



The oxygen deficiency index blueprint allows an economic and quick scan via baseline assessment for forecasting the risk of seasonal oxygen deficiency in the North and Baltic Seas

Authors: Alexandra Marki¹, Xin Li¹, Simon Jandt-Scheelke¹,

5 ¹Federal Maritime and Hydrographic Agency (BSH), Bernhard-Nocht-Str. 78, 20359 Hamburg, Germany

Correspondence to: Alexandra Marki (alexandra.marki@bsh.de)

Abstract.

10 Oxygen deficiency zones (ODZs) in coastal seas can become hazardous to organisms and may have severe ecological and economic consequences for the environment, the fisheries, and the tourism industries. A tight interaction between ventilation and respiration governs marine oxygen levels. Regions with high primary production and a thin water column below the seasonal mixed layer are particularly prone to the formation of oxygen deficiency. In the study of Große et al. (2016) the critical parameters of the oxygen deficiency index (ODI) were identified as stratification and primary production during the
15 formation of oxygen deficiency in the seasonally stratified regions of the North Sea. In order to approach realistic spatio-temporal distributions of ODZs, Große et al. (2016) formulated a depth index serving as a proxy for the thickness of the water column below the mixed layer depth (MLD). Here we propose the further developed ODI to represent two differing hydrographic regimes, the North and the Baltic Seas, by using a density-based criterion of the MLD and the vertical extension of the water column between the seafloor and the bottom layer of the MLD. Moreover, we define the stratification status of
20 the water column using continuous stratification periods of 30 days as our reference period for higher risks of developing ODZs. Different to Große et al. (2016), net primary production is not cumulated over the entire growing season but only over this reference period. With these modifications, the revised ODI offers intuitive, short-term forecasts on the areas at risk of developing oxygen deficiency in high spatio-temporal resolution for the coastal zone of the North and Baltic Seas. This allows an operational forecasting of ODZs to inform responsible authorities and civil services in advance. We propose an economic
25 solution to assess oxygen conditions of the past, the present and test for the risk to developing ODZs in the near future. We are able to run all necessary simulations and calculations for this research on a simple laptop. We mostly used free and open software products and Open Data products. Our data set up consists of: a) Free available netCDF output files of the operational HBM-ERGOM model and b) free available data from the MARNET monitoring network, both operated by the Federal Maritime and Hydrographic Agency (BSH).



30 1 Introduction

Oxygen (O₂) concentration have drastically declined over the last five decades (Breitburg et al., 2018; Oschlies, 2021) caused by a number of effects including anthropogenic climate forcing (Oschlies et al., 2018; Oschlies et al., 2017). Low levels of oxygen are documented for an increasing number of areas including the North and Baltic Seas (Hansson and Viktorsson, 2023). To gain a better understanding of regional oxygen dynamics and their impacts on ecosystem services (Bassett et al., 2019), the oxygen deficiency index (ODI) blueprint can be applied as a first step to forecast the development of Oxygen Deficiency Zones (ODZs). Since biogeochemical and physical processes shape the environment of marine ecosystems, a disequilibrium amongst those processes, especially in coastal and shelf seas, may cause severe environmental threats and economic impacts to the fisheries and the tourism (Laffoley and Baxter, 2019). For example, potentially harmful events, such as excessive algae blooms followed by low oxygen conditions and/or hypoxia can cause fish-kills. Low bottom oxygen is also harmful to sedentary benthic and demersal organisms, since most of them cannot escape hypoxic areas (Pörtner and Knust, 2007; Levin and Gallo, 2019). Although oxygen is essentially a “by-product” of plants’ photosynthesis, it is vital for oxygenic respiration and metabolic processes of living organisms on our planet, above and underwater (Pörtner and Knust, 2007). In 2003, the Oslo and Paris (OSPAR) Commission defined low oxygen (O₂) conditions by O₂ concentrations of 6 mg O₂ L⁻¹ (187.5 μmol L⁻¹) or below. Pörtner and Knust (2007) suggested that even higher concentrations than the OSPAR threshold may harm marine organisms. It is thus necessary to gain a better understanding on the drivers and processes that determine the risks of developing ODZs now and for a future (Oschlies et al., 2017; Breitburg et al., 2018; Oschlies et al., 2018) with decreased marine oxygen availability.

Conditions that may lead to the development of ODZs in the North- and Baltic Seas are sluggish ventilation, stratification, and excessive sinking out of organic material to the seafloor due to enhanced primary production (Hansson and Viktorsson, 2023). Shallow coastal waters are often intermittently stratified, creating a vertical layering of the water column, as a result of the formation of vertical gradients in density (a function of temperature and salinity and/or stratification due to high load of organic matter (Huthnance et al., 2022)). Especially in onshore and near-coastal regions, the low-oxygenated, denser offshore waters remain near the seafloor (Huthnance et al., 2022). Sediment respiration favours rapid oxygen depletion of this so-called ‘hypoxic carpet’ (Carstensen and Conley (2019)). Very often, a persistent pycnocline limits the export of oxygen down to the bottom mixed layer (BML). As long as this condition is maintained, very limited/little exchange with the water-layers above will occur until stratification erodes.

Große et al. (2016) first proposed an indicator for the risk of the formation of oxygen deficiency in the North Sea. They identified three key factors governing the formation: continuous water column stratification as a prerequisite preventing ventilation, autochthonous organic matter (i.e., from primary production) and its sinking as the main reason for O₂ consumption. The authors determined the duration of the stratification period, primary production and bottom depth as the



key parameters to define an oxygen deficiency index (ODI) for the North Sea. Bottom depth served as a proxy for the thickness of the water column below the MLD.

Here we adapt the formulation of these key parameters in order to represent the North and include the Baltic Seas which harbours distinct environmental characteristics. Circulation in North Sea to the north-western side of Germany is dominated by tides and has an open connection to the Atlantic Ocean via the English Channel and the Norwegian Seas. Temperature differences between the warm water from the English Channel meeting with the cold oceanic waters advected from the Nordic Seas, are the main cause for stratification. However, high salinity waters might flow inshore, whilst low salinity waters might flow offshore, generating also counter directed currents and influence hydrodynamics particularly where these two-ocean currents meet each other. Conversely, the intra-continental character of the Baltic sea is rather non-tidal and connected to the North Sea only by narrow passages through the Danish sounds and Danish Strait (Zeiler et al., 2008). Moreover, the Baltic Sea shows salinity gradients from the North to the South and one from the West to the Eastern Baltic Proper. Those shifts in salinity are said to be the main reason there for stratification and prevent ventilation of the deep waters. (Hansson and Viktorsson, 2023). As stated by Hansson and Viktorsson (2023), Major Baltic Inflows (MBI) of oxygenated North Sea waters became rare in the last years. Only if the water volume and the density of the MBI is large enough to bypass the shallow sills of the several Baltic basins, oxygen-rich waters may sink to the bottom and (re-)supply O₂ to the oxygen-depleted bottom waters (Hansson and Viktorsson, 2023).

As for the North Sea and for the Baltic Sea, the consequences of ODZs on the ecosystem should also take into account the frequency and the duration of ODZs. In addition, ODZs should also be considered in terms of their intensity and spatial extent. To determine latter ones, we need both, temporally and spatially highly resolved data. Although the observational data availability from environmental monitoring has improved over the last years, measurements still lack sufficient temporal and spatial coverage to fully represent variability across different temporal and spatial scales. A good and economic solution to address this limitation is the comparison of ecosystem model outputs with ‘real’ observational monitoring data.

We apply the operational model system of the Federal Maritime and Hydrographic Agency (BSH; (Brüning et al., 2014; Brüning et al., 2021; Neumann, 2000) to display modelled bottom oxygen. We further developed for both regimes, the North Sea and the Baltic Sea, the ODI (Große et al. (2016) to determine the temporal and spatial distribution of ODZs. To validate our (forecasting/hindcasting) ODI output(s), we compare our ODI calculations against the near real time Marine Environmental monitoring network (MARNET) observational data on six stations in the North Sea and four stations in the Baltic Sea (Table 1, Marnet (2018-2023). The accuracy of our ODI output may in future help to identify the area, spread and temporal evolution of ODZs, which may assist the planning of research cruises and periodical sampling.

Our modified ODI addresses the following limitations of the HBM-ERGOM model: Foremost, the operational BSH model system is limited to 120-h-forecasts due to the limited forecast length of reliable meteorological forcing data. Besides that, we wanted a procedure, which is independent of specific model versions and types. Therefore, we developed an independent tool,



the ODI (blueprint) toolbox, that neither interfere with the model's source code, nor required development as an additional compulsory module of HBM-ERGOM.

95 Additionally, we were looking for a fast application and simple analyses, reproducing interpretable, reliable results. Within the framework of a broader application, we further aim for comparable results amongst different environmental regimes. As such, system insights can help to identify dynamic tendencies and critical tipping points, which as a result might help to choose points for action. Moreover, we see the potential of the ODI to forecasting the risk of developing ODZs in the near future in our seas, which are not covered yet by the current monitoring platforms. In addition, all this may mean that the parameter set-up in ecosystem models can be better narrowed down and constrained in future. Just like the temporal and spatial dependencies and time scales of biogeochemical cycles, such as sinking out of organic matter and remineralisation at the seafloor.

2 Methods

2.1 Development of a common Mixed Layer Depth (MLD) formulation for the North and Baltic Seas

Since salinity is a key control of stratification in the Baltic Sea, we had to adapt the ODI calculation of Große et al. (2016) by employing an MLD criterion accounting for both temperature and salinity, making it applicable to both the North and the Baltic Seas. Thus, we decided to use the density-based criterion after De Boyer Montégut et al. (2004). Their criterion is defined as a threshold value of temperature ($\Delta T = 0.2 \text{ }^\circ\text{C}$) or potential density ($\Delta \sigma_\theta = 0.03 \text{ kg m}^{-3}$) from a near-surface value at a reference depth ($Z_{ref} = 10 \text{ m}$). This means that the MLD is situated at the deepest water column layer, where the density difference between the local potential density and the potential density at 10 m water depth is less than 0.03 kg m^{-3} . Moreover, we implemented the MLD formulation according to Millero and Huang (2009) by applying the corrected values in the corrigendum according to Millero and Huang (2010).

2.2 Modification of the Oxygen Deficiency Index (ODI)

All quantities for the ODI calculation are extracted from the operational HBM-ERGOM model output. The ODI stays within the range of 0 to 1, with values close to 1 indicating a high risk of oxygen deficiency formation, whilst values closer to 0 indicate a low probability that an ODZ will form.

The modified ODI equation for the forecast day for each grid cell, similar to the original one (Große et al. (2016), combines three core indices: the stratification Index (I_{strat}), the depth index (I_{depth}) and the net primary production index (I_{NPP}). The ODI assumes that stratification (represented by I_{strat}) is the necessary prerequisite for an ODZ to form, while the combination of the water column thickness below the MLD (represented by I_{depth}) and the organic matter production



(represented by I_{NPP}) eventually determine whether O₂ deficiency occurs. We then apply I_{strat} to the weighted sum of I_{depth} and I_{NPP} which equals the numerical value 1.

The formula of the ODI in its current version reads as

$$ODI(x, y, t_0) = \sum (w_{depth} I_{depth}(x, y, t_0), w_{NPP} I_{NPP}(x, y, t_0)) * I_{strat}(x, y, t_0), \quad (1)$$

125

We choose one formulation within the overall highest correlation coefficients between the bottom-oxygen model output and the calculated ODI by considering the fine temporal resolution of the ODI. Like this we defined the weights of 1/3 for I_{depth} and 2/3 for I_{NPP} and obtained our ODI33rev configuration.

This formulation is now applied to compare the observed sensor-based oxygen concentrations and the ODI: We considered
130 time series ranging from 1st January 2018 until 31st December 2022, thus a total of five years for both regimes. Correlation coefficient values close to -1 indicate the highest agreement between deepest sensor oxygen saturation and the ODI at the platforms of Table 1 and Table 2. During the course of this research, we tested several set-ups, which are shown in the supplements section. The ODI33rev configuration is presented here as an example in this study.

135 2.3 Three subindices of the ODI

According to the key parameters to calculate the ODI defined by Große et al. (2016), we further extended the three subindices, given by the stratification index (I_{strat}), the depth index (I_{depth}) and the net primary production index (I_{NPP}). The ODI by Große et al. (2016) was originally developed only for hindcasts and nowcasts. In contrary to our modified ODI Toolbox, which is applied in the operational mode to forecasting the development of ODZs. Therefore, we had to adjust stratification
140 index, depth index and net primary production index as outlined below.

2.3.1 Stratification Index (I_{strat})

For each model grid and each day within the period $[t_0 - \Delta t_{ref}, t_0]$, where we define the length of Δt_{ref} with 30 days and t_0 as our forecasting day, the stratification status of the water column is determined using the density-based criterion (to account for the effects of T and S on stratification), with $t \in [t_0 - \Delta t_{ref}, t_0]$.

145 The stratification index over the reference period is calculated:

$$I_{strat}(t_0, \Delta t_{ref}) = \frac{1}{\Delta t_{ref}} \int_{t_0 - \Delta t_{ref}}^{t_0} I_{strat}^*(t) dt, \quad (2)$$



We also define the water column as stratified (I_{strat}^*), if, first of all more than one MLDs are present in the water column and additionally the index of the deepest MLD layer, hereafter called Bottom Mixed Layer Depth (BMLD) is smaller than the index of the modelled bathymetric bottom layer. The BMLD corresponds to the bottom layer of the pycnocline.

$$I_{strat}^*(t) = \begin{cases} 1 & \text{if stratified} \\ 0 & \text{otherwise} \end{cases}, \quad (3)$$

150

Equation (1) accounts only for the total number of days when the water column according to Equation (2) over the reference period is stratified. If an extended period of continuous stratification is replaced by a shorter period of continuous non-stratification directly prior to a date within the forecast, the water-column might still be stratified, or, in the case of sporadically extreme events, i.e., storm-surges, it might not. Thus, we also have a look into short-term events, prior to a date within the forecast, and we calculate the final stratification indexes over two different reference periods. We consider a shorter reference period given by 10 days prior to a specific date and a longer reference period represented by 30 days prior to that date. This approach might also help to consider the effects on water column stratification in the case of extreme mixing events, directly prior to a date within the forecast, especially in more dynamical and shallower water, which helps to prevent overestimation of I_{strat} . Combining these two indices, the stratification index for the forecast day is the minimum of both:

155

160

$$I_{strat}(t_0) = \min(I_{strat}(t_0, 10), I_{strat}(t_0, 30)), \quad (4)$$

2.3.2 Depth index (I_{depth})

For the calculation of the depth index (I_{depth}) we only include the stratified days when $I_{strat}^*(t) = 1$ in order to prevent (implicit) double-accounting of stratification in both I_{strat} and I_{depth} . It should further be noted that this formulation also implies $0 \leq I_{strat}(t_0) < 1$. Moreover, we point out that the occurrence of the MLD being smaller than the water column depth (H), implies $MLD(t) < H$.

To fulfil these conditions, we are introducing the critical thickness (D_{crit}), where $I_{strat}^*(t) = 1$ and $D_{crit} = 1$ m. The critical thickness only allows for a maximal depth index ($I_{depth} = 1$), if the difference between the bathymetric bottom depth and the BMLD is $\leq D_{crit}$.

170



The depth index is given as

$$I_{depth}^*(t) = \frac{\min(H - D_{crit}, MLD(t))}{H - D_{crit}} \cdot I_{strat}^*(t), \quad (5)$$

The depth index for the forecast day within the reference period is given by:

$$I_{depth}(t_0, \Delta t_{ref}) = \frac{1}{\Delta t_{ref}} \int_{t_0 - \Delta t_{ref}}^{t_0} I_{depth}^*(t) dt, \quad (6)$$

175 2.3.3 Net primary production index (I_{NPP})

In order to check for the potential to forecast the development of ODZs, we changed the formulation of I_{NPP} . The net primary production (NPP) index for the forecast day is derived from the time-averaged NPP

$$\overline{NPP} = \frac{1}{\Delta t_{ref}} \int_{t_0 - \Delta t_{ref}}^{t_0} NPP(t) dt, \quad (7)$$

and the NPP integrated over the whole water column (z),

$$NPP(t) = \int_{-H}^0 NPP(t, z) dz, \quad (8)$$

180 then reads as:

$$I_{NPP}(t_0) = \max\left(0, \min\left(1, \frac{\overline{NPP} - NPP_{min}}{NPP_{max} - NPP_{min}}\right)\right), \quad (9)$$

For NPP_{min} and NPP_{max} , we use the minimum and maximum over the reference period at each model grid. Variations of I_{NPP} calculations are in the Supplements. Variations were applied in different test suites for different needs to determine ODZs, e.g., hindcasts, seasonal hindcasts, special areal forecasts and similar.

185 2.4 Operational Model HBM-ERGOM

This study is based on the physical HIROMB-BOOS (HBM) model coupled to the biogeochemical ERGOM model (Ecological ReGional Ocean Model, (Neumann, 2000)) at the Federal Maritime and Hydrographic Agency (BSH). The setup and validation of the (free-run) operational model system has been published by Brüning et al. (2021) and on the BSH website (https://www.bsh.de/DE/THEMEN/Modelle/modelle_node.html). The BSH model system consists of two two-way nested
 190 grids. The coarse grid with up to 36 vertical layers and a horizontal resolution of 3 nautical miles covers the North Sea and Baltic Sea from approximately 4°W to about 30°E, with the North Sea from approximately 49.5°N to about 61°N and the



Baltic Sea from approximately 53°N to about 65.5°N. The fine grid with up to 25 vertical layers and a horizontal resolution of 0.5 nautical miles covers the German coastal waters, defined as area roughly between 6°E to 15°E and 53°N to 56.5°N. Although the total number of the vertical layers differs, the vertical resolution of both grids is identical (Brüning et al., 2014; 195 Brüning et al., 2021). Thus, for simplicity and performance speed we merged the fine and the coarse resolution grids into one common grid, resulting in 25 common depth levels. The ERGOM model was originally developed by Neumann (2000) for the Baltic Sea but has been adapted for the application to the North Sea (Maar et al., 2011). In its current version at the BSH, ERGOM runs with 15 prognostic state variables and calculates diagnostically chlorophyll *a*, Secchi depth, pH and pCO₂ (Doron et al., 2011; Doron et al., 2013; Neumann et al., 2015). ERGOM also contains a module for carbon and total alkalinity 200 after (Schwichtenberg et al., 2020). The operational bio-geochemical model output also includes the oxygen concentration. Oxygen saturation as well as the extracted bottom oxygen saturation and bottom oxygen concentration are derived via postprocessing routines. We used the bottom oxygen tracers to estimate the overall performance and dynamics of the ODI formulations. We fed the ODI calculations with netCDF output files of HBM-ERGOM, where we extracted vertical profiles of salinity and temperature to calculate the MLD. Moreover, we used simulated net primary production that feeds into I_{NPP} 205 index.

2.5 MARNET monitoring data

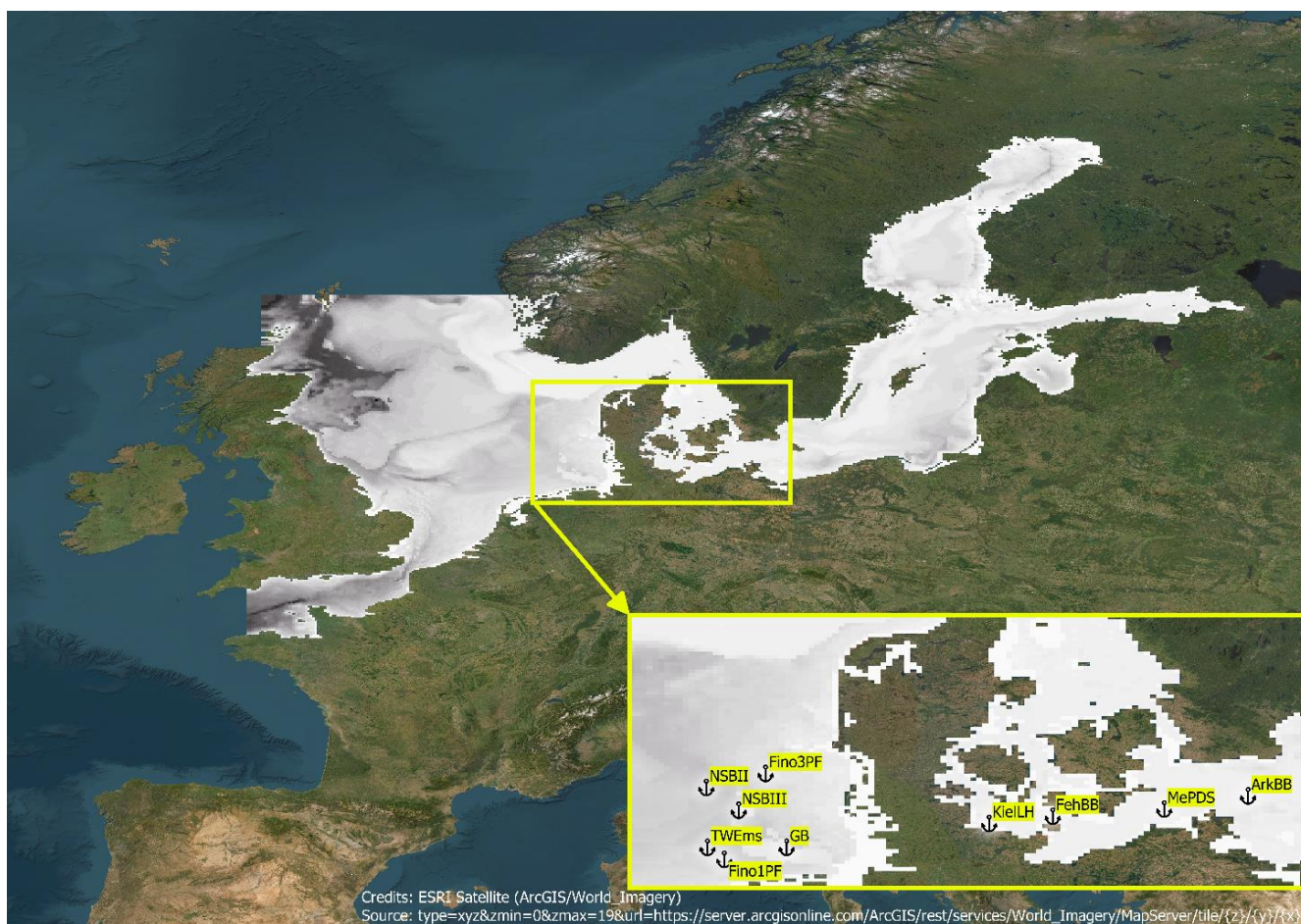
For our analysis presented here, we compare near-bottom oxygen saturation of six sensor-based measurement platforms in the North Sea and four in the Baltic Sea, shown in Figure1 and Table 1. Datasets (Marnet, 2018-2023) in netCDF format were 210 downloaded from MARNET (https://www.bsh.de/DE/DATEN/Klima-und-Meer/Meeresumweltmessnetz/messnetz-marnet_node.html) and missing observational data might be due to maintenance, and/or malfunction of the platform and/or the sensor. Thus, for processing the dataset we filtered each station for potential outliers and unreasonable data. In the following, we only consider oxygen saturation data with a quality flag = 1 (good date) and quality flag = 2 (probably good data). We chose the deepest sensor measurement point in accordance with this data selection (Table 1). Since the datasets come 215 in hourly measurements, observations were condensed to daily means beforehand. Unfortunately, none of the stations covered all days within the whole timeseries period, 1st January 2018 until 31st December 2022, although Kiel Lighthouse (KielLH) delivered good data coverage over five years. Furthermore, we chose the stations, that hinted at three seasonal events. Preselection and data aggregation was done with CDO (Climate Data Operators version 2.0.4; <https://mpimet.mpg.de/cdo>) and Python (versions 3.10 and 3.11.).

220



Table 1: Marine Environmental monitoring network (MARNET) operated by the BSH used for validation. Five stations for the Baltic Sea and six stations for the North Sea; sensor 1 depth is deepest depth with evaluable oxygen concentration data. Observational Data (Marnet, 2018-2023) have been collected from the (https://www.bsh.de/DE/DATEN/Klima-und-Meer/Meeresumweltsmessnetz/messnetz-marnet_node.html).

Station	Latitude	Longitude	Platform Name	Region	Depth s1 (sensor 1)
MePDS	12.7°E	54.7°N	Measuring Pile Darss Sill	Baltic Sea	19 m
ArkBB	13.867°E	54.883°N	Arkona Basin Buoy	Baltic Sea	40 m
FehBB	11.15°E	54.6°N	Fehmarn Belt Buoy	Baltic Sea	24 m
KielLH	10.267°E	54.5°N	Kiel Lighthouse	Baltic Sea	13 m
FinoPF1	6.583°E	54°N	FINO1 Platform	North Sea	25 m
FinoPF3	7.158°E	55.195°N	FINO3 Platform	North Sea	18 m
NSBII	6.333°E	55°N	North Sea Buoy II	North Sea	35 m
NSBIII	6.783°E	54.683°N	North Sea Buoy III	North Sea	35 m
TWEms	6.35°E	54.167°N	Unmanned Lightship TW Ems	North Sea	30 m
GB	7.45°E	54.1667°N	Unmanned Lightship German Bight	North Sea	30 m



230

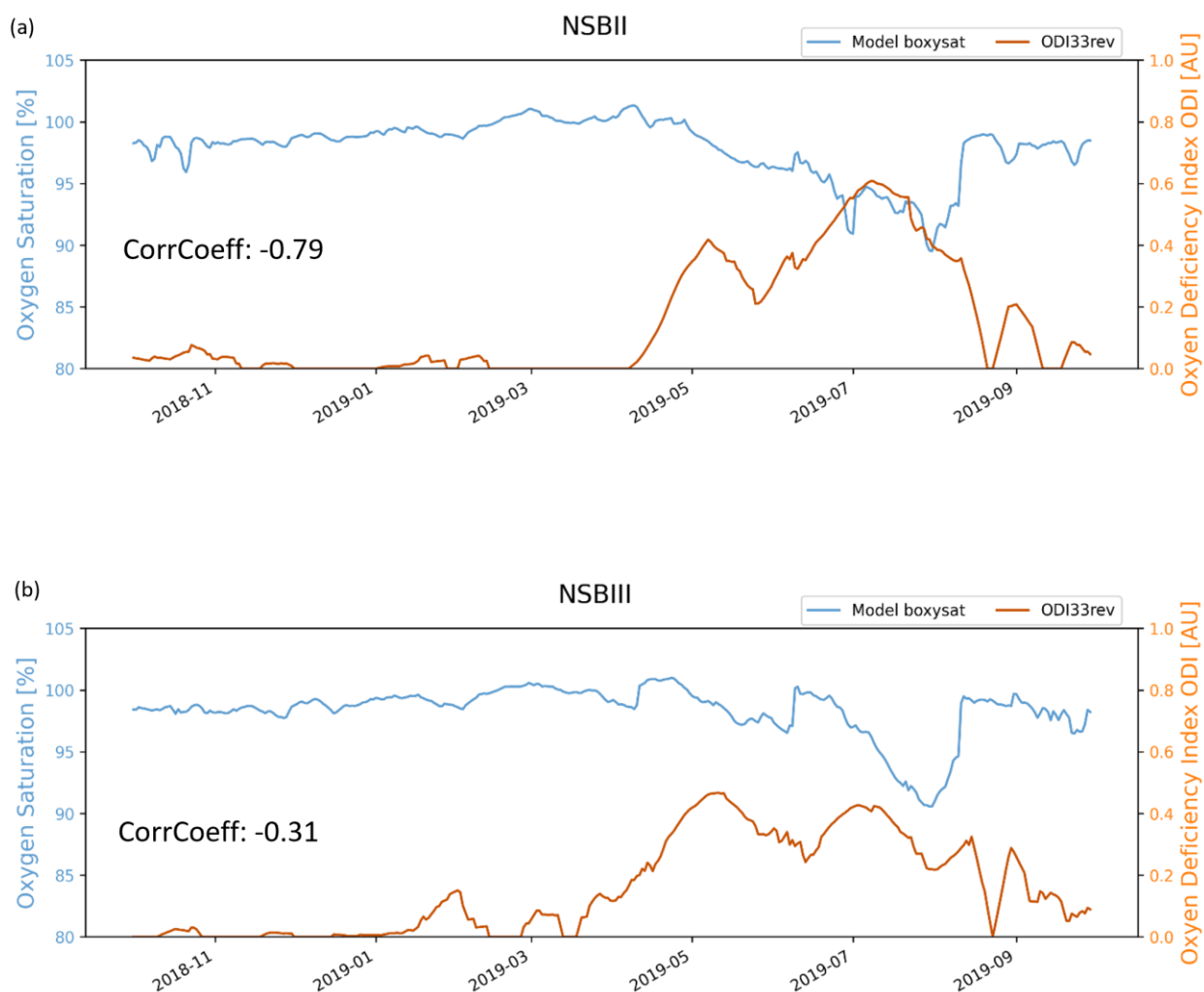
Figure 1: Map of the study region. The greyish area, is showing approximately the whole model domain of the HBM-ERGOM, ranging from the North Sea to the Baltic Sea; framed yellow box with arrow zooming approximately into the area, to show the location of the six platforms/stations in the North Sea and four stations in the Baltic-Sea used for validation (Table 1). Graphics were made using QGIS, basemap; credits to ESRI Satellite (ArcGIS/World_Imagery).

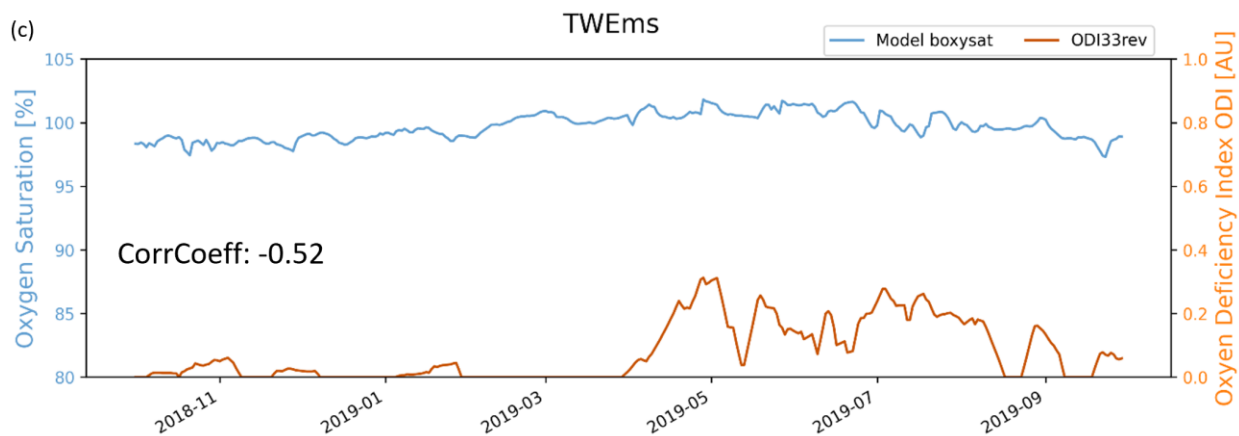
2.6 Data analyses and statistics

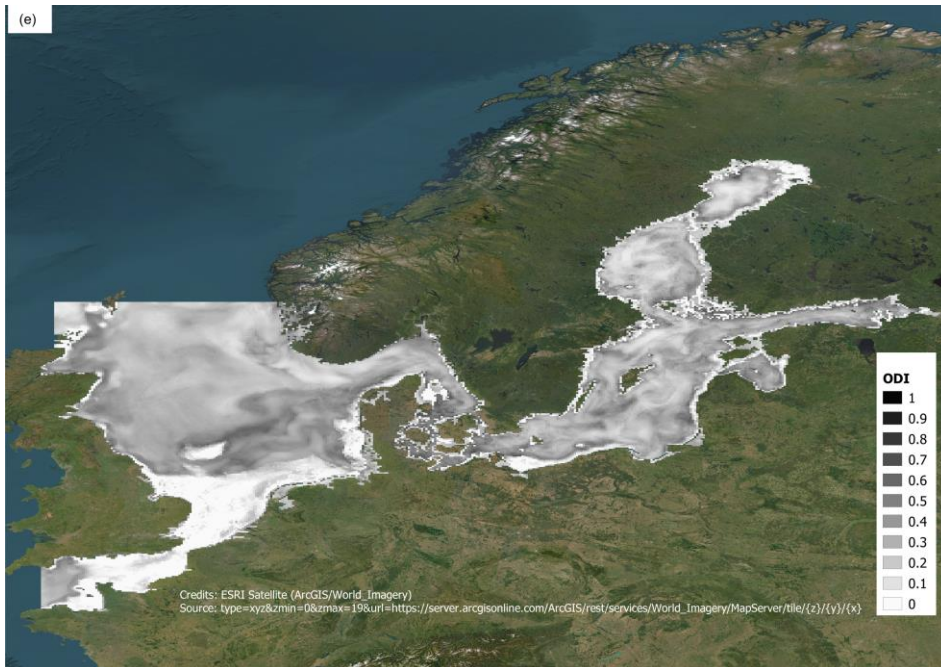
Pre-calibration of the ODI calculations and validation therein was done with the HBM-ERGOM model products of bottom oxygen saturation (boxy_sat, Figure 2) and bottom oxygen concentration (not shown here), as well as net primary production (NPP; Figure 3) and calculated mixed layer depth (MLD; Figure 4). We calculated the correlation coefficients between the ODI and the modelled bottom oxygen saturation at three stations in the North Sea (NSBII, NSBIII and TWEmS, Figure 2a-c) in the period between 1st October 2018 and 30st September 2019. The bottom oxygen saturation calculated with HBM-ERGOM



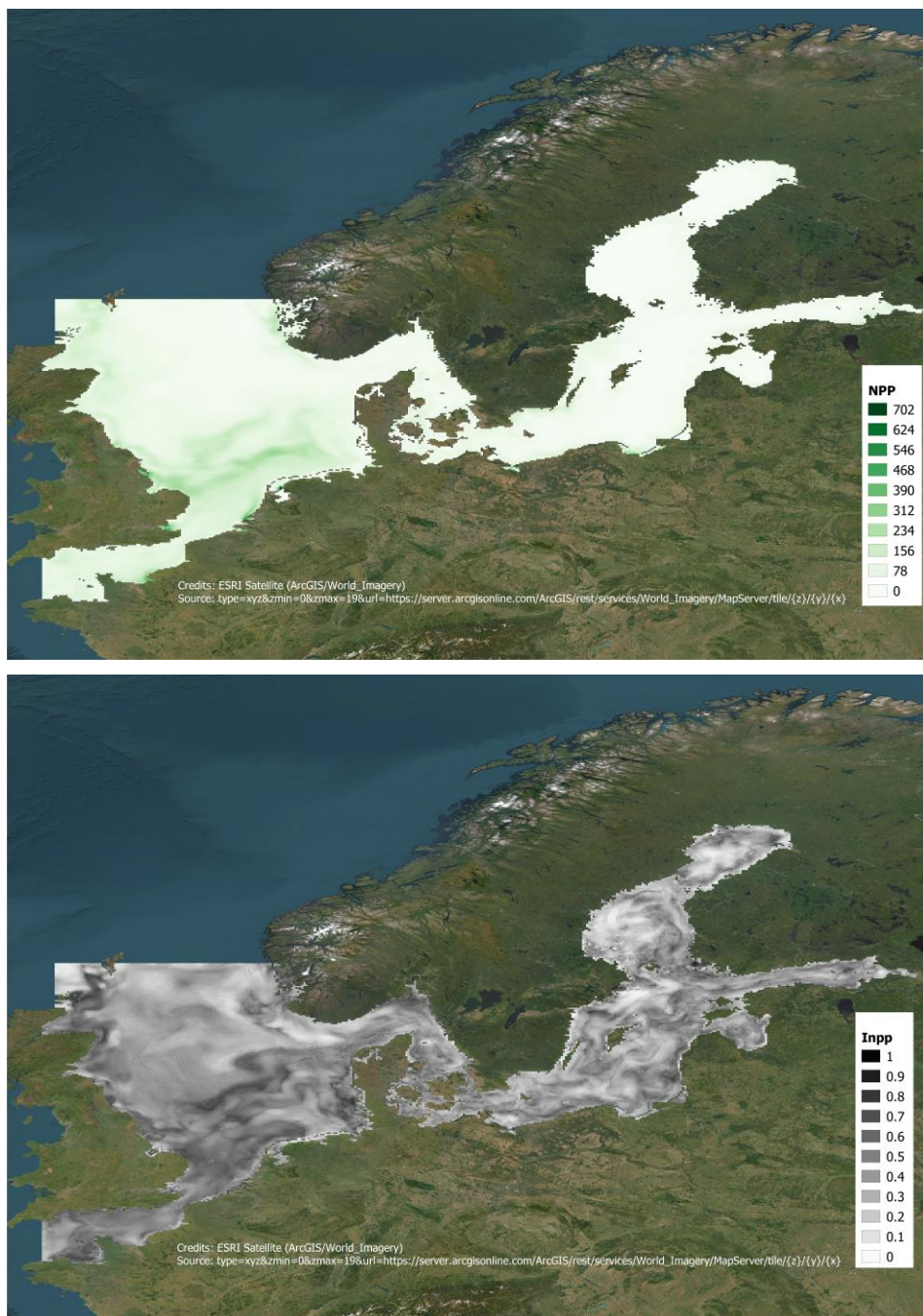
shows the low and high oxygen values in a proximity to the bottom layer, which is defined as the last depth level at each grid cell according to the bathymetry of the model (Figure 2d). Overall, the calculated ODI corresponds well with the Oxygen
240 zones, where low ODI values toward 0 correspond to higher bottom saturation values indicating a lower risk for developing ODZs (Figure 2e).







250 **Figure 2: Panel a-c: Comparison of modelled bottom oxygen saturation with the ODI33rev showing Pearsons Correlation Coefficients in the period of 1st October 2018 to 30th September 2019); Panel d: HBM-ERGOM modelled bottom oxygen saturation – the results are rounded down to the next lower integer value; with panel e: Oxygen Deficiency Index (ODI), values close to 1 show higher probability of developing an ODZ and vice versa; (simulation day: 8th August 2021).**



255 **Figure 3: Comparison of - top panel: HBM-ERGOM modelled net primary production (NPP [$\text{mg m}^{-3} \text{d}^{-1}$]) – values are vertically integrated over the whole water-column at each grid-cell and the results are rounded down to the next lower integer value; with bottom panel: net primary production index (INPP), values close to 1 show higher probability of higher NPP and vice versa; (simulation day: 8th August 2021).**





265 **Figure 4: Comparison of - top panel: calculated mixed layer depth (MLD) – the results are rounded down to the next lower integer value; middle panel: stratification index (I_{strat}), values close to 1 show higher probability of developing stratification and vice versa; bottom panel: the depth index (I_{depth}) represents the water column thickness below the MLD and is given inter alia by the product of the MLD and I_{strat} ; (simulation day: 8th August 2021).**

After the pre-calibration we started to calibrate different ODI configurations over a 5 years timeseries and compared the calibrations to the modelled bottom oxygen saturation and near real time data of the MARNET stations shown in Table 1. We calculated the Pearson's Correlation Coefficient over the complete timeseries, by considering only the prefiltered available data points. This has been done for simplicity due to the scarcity of data, we run the statistic if we had at least 10% of valid datapoints regarding to the whole timespan of the timeseries (1st January 2018 until 31st December 2022). In the supplement we show the correlation coefficients of both sensors over the whole range of ODI setups at all monitoring stations (Supplement Tables 2,3, 5,6 and Figures therein) according to Supplement Table 1.

275 Nevertheless, calculating statistics for shorter time periods within the one-year period has a significant impact on the correlation coefficients. In the supplement we show the effect of annual statistics on the different ODI configurations at KielLH platform considering all time-lags (Supplement Figure 2,3 and Supplement Table 4) and smaller sampling sizes, i.e., just one summer season per year, can rise significantly the relationship between the parameters in question (not shown here, Marki in prep.). Here we mainly focus on the agreement of 2 seasonal patterns, for simplicity hereafter called winter- and summer season. The winter (November to February) and the summer (March to October) season and/or cyclic patterns between the



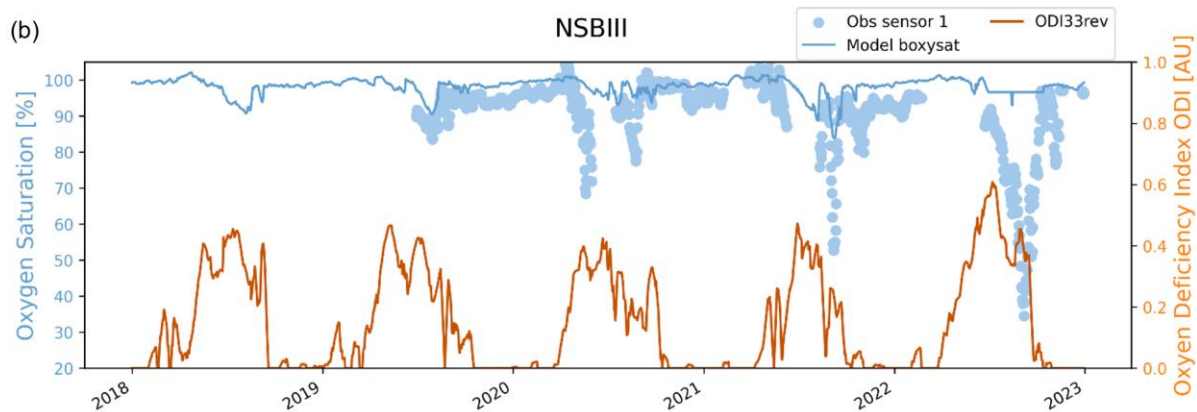
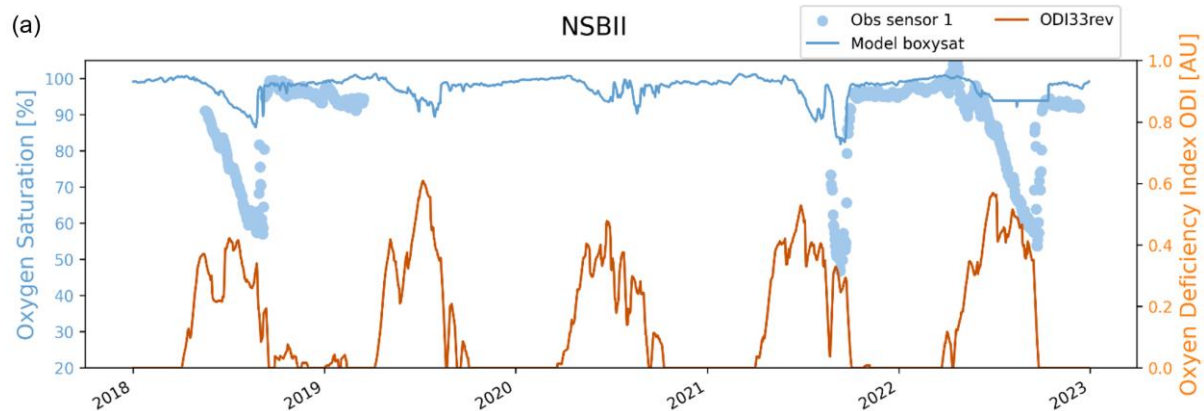
280 ODI and the sensor based near bottom oxygen saturation measurements. Both seasonal trends, in the winter with low and in
the summer with high oxygen saturation values shown in the observations can be found in the ODI at all stations (Figure 5a-
f). ODI values close to 0 indicate a low risk, whilst ODI values close to 1 indicate a high risk of developing an ODZ (Figure
5a-f). A negative correlation coefficient (r) between the ODI and the observations significate that, with declining measured
oxygen saturations the ODI values will raise and the risk of developing a ODZ becomes higher, and vice versa. In contrary, a
285 positive correlation coefficient indicates that with declining oxygen saturations, the ODI values will also decline. The further
away the correlation value (r) between the ODI and the measurements, the stronger is the relationship between these two
parameters.

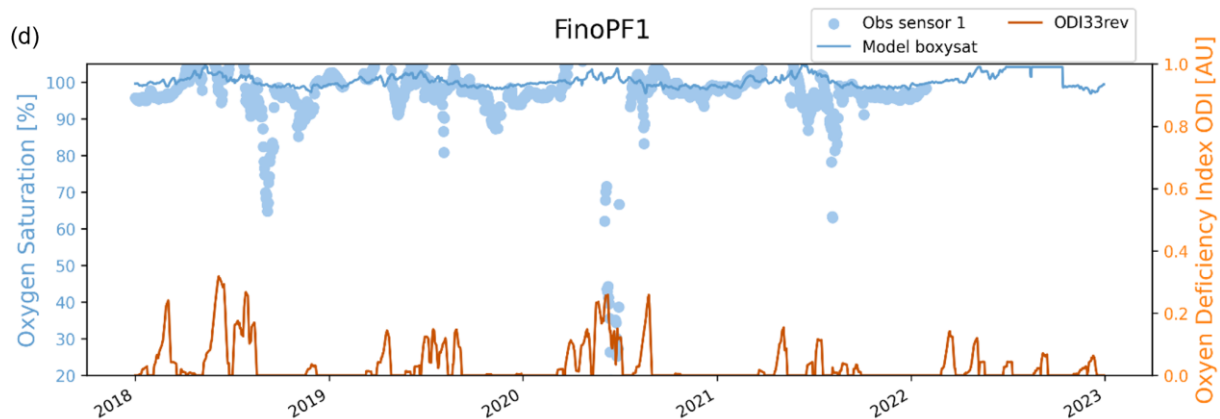
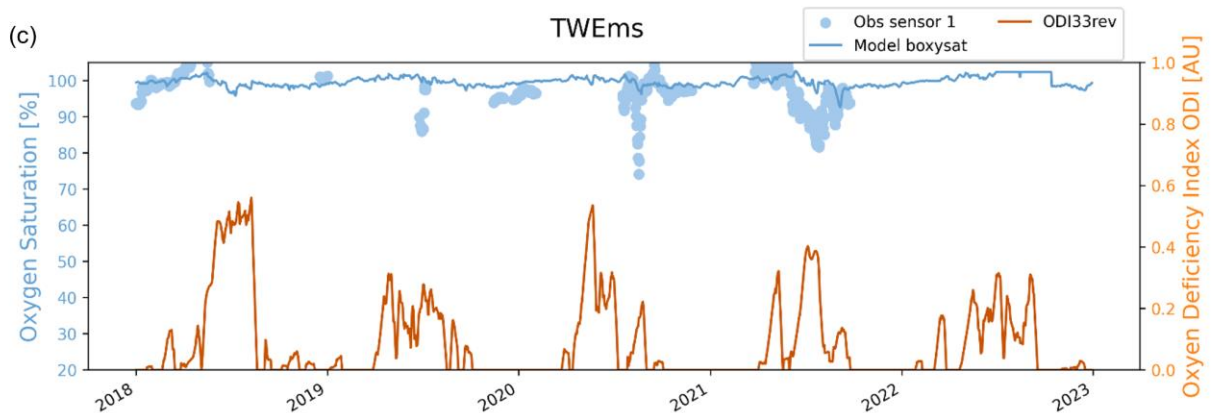
Data statistics and data visualisation was performed in Python (v 3.11.x) using the Python packages numpy (v 1.25.x) and
pandas (v 2.0.x)

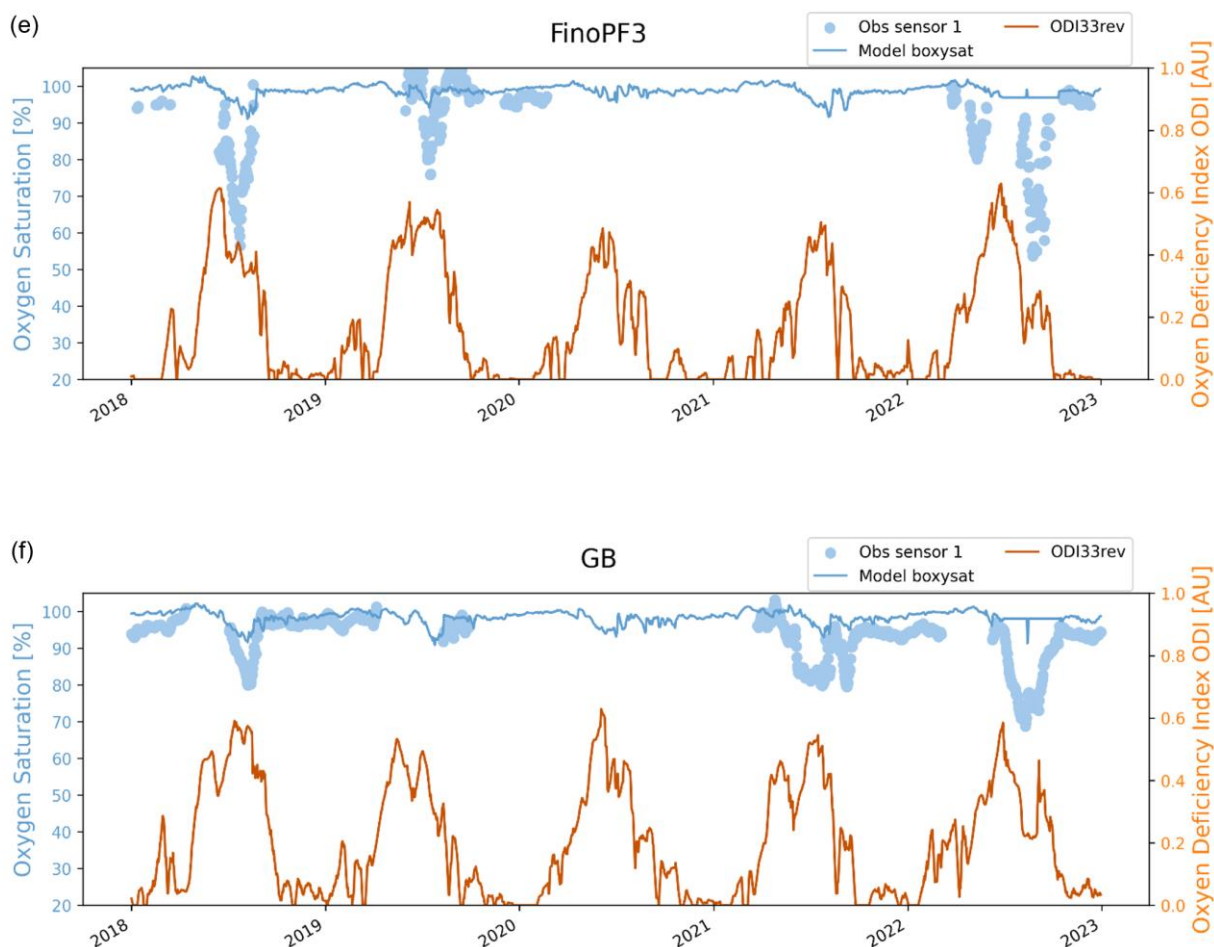
290 3 Results

3.1 North Sea

At each of the six MARNET stations in the North Sea, the ODI clearly displays two main seasonal patterns. In winter season,
at each station the oxygen saturation is higher than in summer. Summer season oxygen deficiency can reach levels below 30%,
as on platform NSBII and FinoPF1. The ODI displays very well the pattern of both seasons (Figure 5a-f), except at FinoPF1
295 with ODI values barely reaching 0.2 (Figure 5d), and a very weak negative correlation coefficient between the ODI and the
observed oxygen saturation ($r = -0.058$; Table 2: lag0). Moreover, the lowest oxygen saturation in the year 2020 was not
captured by the ODI. In contrary, the ODI seems to capture quite well the Oxygen dynamics at FinoPF3 Figure 5e), although
the measurements are rather scarce Oxygen saturation at NSBII and NSBIII, is reproduced by the ODI very well (Figure 5a,b),
especially the lowest oxygen concentration at the end of the summer season in 2022 at station NSBII (Figure 5a). Moreover,
300 platform NSBII has a good negative correlation coefficient ($r = -0.636$; Table 2: lag0) whilst NSBIII owns a moderate
correlation coefficient ($r=-0.475$; Table 2: lag0). At platform GB the ODI seems to overestimate the risk of developing an ODZ
(Figure 5f), although the negative correlation coefficient is moderate ($r=-0.483$; Table 2: lag0). Platform TWEmS has the
fewest measurements of all platforms, however, the seasonality is reproduced with the ODI and peaks of lowest Oxygen
saturation measurements can still be identified (Figure 5c). Generally, at first sight it looks like that the seasonal and/or cyclic
305 ODI timeseries always seems to be ahead of the measurement timeseries (Figure 5a-f).







310

315

Figure 5: Comparison of daily averaged oxygen saturations at deepest sensor depths (sensor1) and modelled bottom oxygen saturation (at the deepest depth layer of the model) with the Oxygen Deficiency Index (ODI) over five years; Timeseries starts at 1st January 2018 and ends 31st December 2022; North Sea stations (a) NSBII, (b), NSBIII, (c) TWEmS, (d) FinoPF1, (e) FinoPF3, (f) GB according to Table 1; all data for observations taken from MARNET (https://www.bsh.de/DE/DATEN/Klima-und-Meer/Meeresumweltmessnetz/messnetz-marnet_node.html); all model simulations from the operational HBM-ERGOM model at the BSH (https://www.bsh.de/EN/TOPICS/Operational_modelling/Ecosystem/ecosystem_node.html); lack of data might be due to maintenance and/or malfunction of the platform and/or sensor.

3.2 Baltic Sea

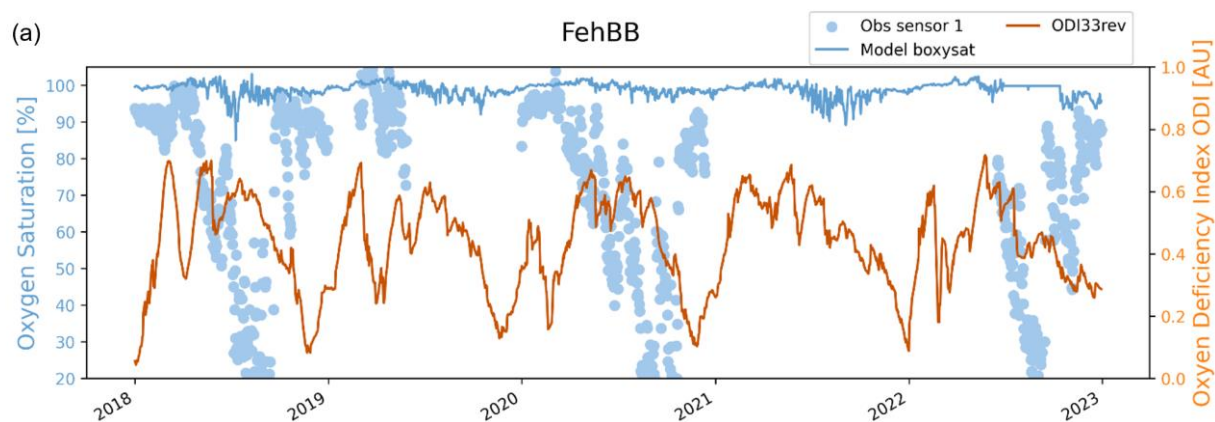
320

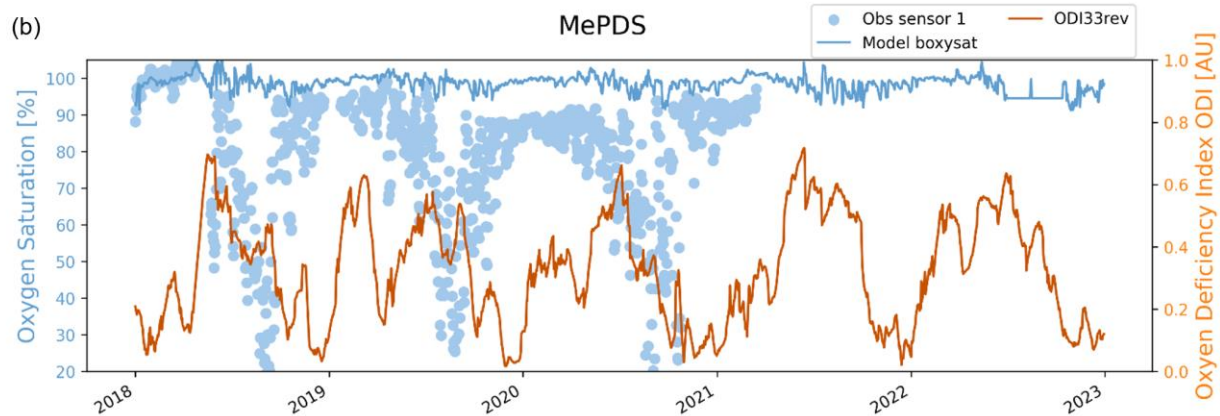
The seasonal trends clearly shown in the observations at station FehBB and MePDS, are reproduced by the ODI rather as cyclic trends, but both showing also lowest values towards the end of each year (Figure 6a, b, respectively). Both stations



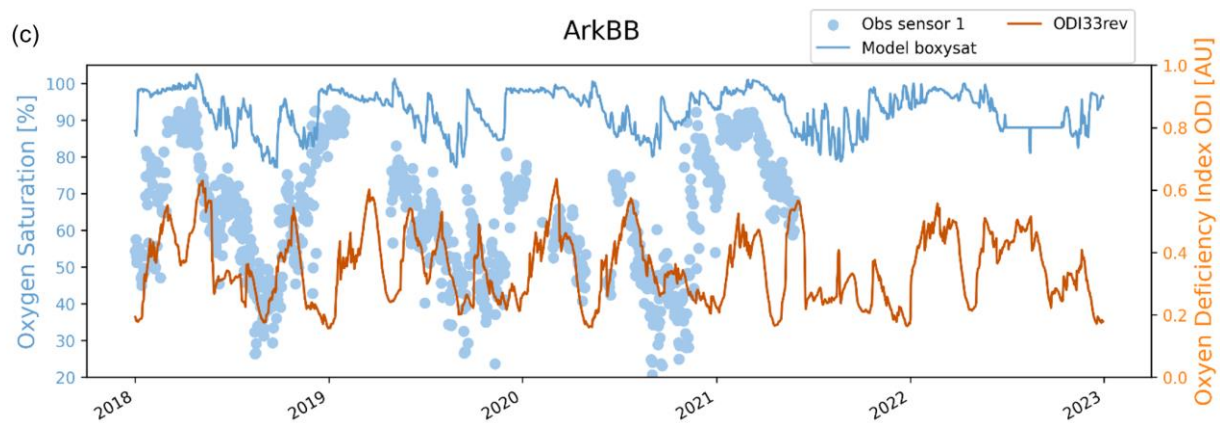
exhibit a rather low but negative correlation, FehBB: $r=-0.35$ and MePDS: $r=-0.32$, between the observations and the ODI (Table 2: lag0). ODI levels around -0.7, indicating a rather high risk of developing an ODZ.

In contrast, the seasonal cycle of KielLH is very prominent and appears clearly in the observations, as well as in the ODI (Figure 6d). Highest ODI values close to -0.8 (high risk) and values close to 0 (low risk), correspond to low and high oxygen saturation levels in the observations, respectively (Figure 6d), whilst showing a moderate negative correlation of $r = -0.39$ between the ODI and the observations (Table 2: lag0). Although the Arkona Basin Buoy (ArkBB) measurement show seasonal trends, the ODI shows rather cyclic trends, that are the strongest amongst all platforms with almost four - winter, spring, summer, autumn - seasonal peaks/year (Figure 6c). Therefore, the correlation coefficient is also weak ($r = -0.16$; Table 2: lag0). Moreover, ArkBB is the only platform having a positive correlation between the ODI and the observations (Table 2: lag0). Moreover, at ArkBB the ODI never reaches 0 and seldom reaches 0 at MePDS, FehBB, pointing towards permanent Oxygen depletion at the bottom layers (Figure 6a,b,c). Also in the Baltic Sea, it looks like that the seasonal and/or cyclic ODI dynamics seem always be ahead when compared to the measurements (Figure 6a-d).





335



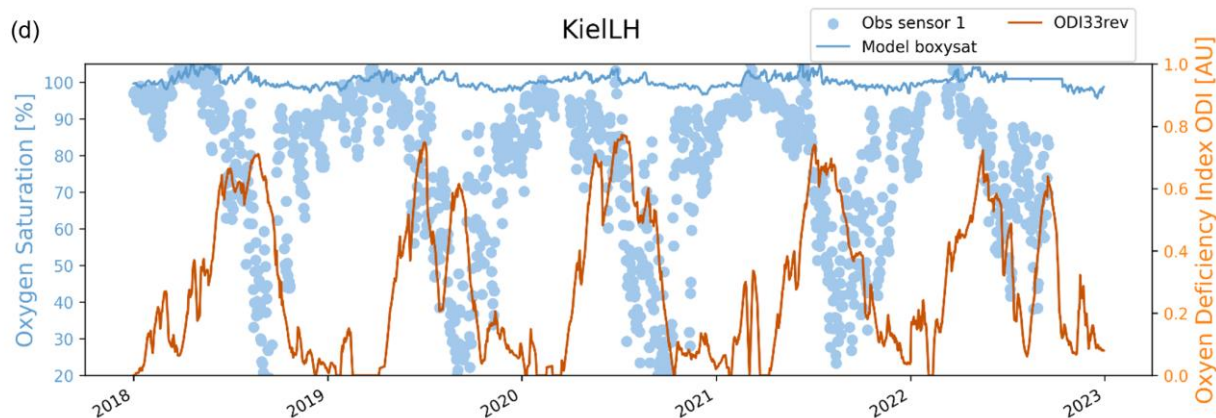


Figure 6: Comparison of daily averaged oxygen saturations at deepest sensor depths (sensor1) and the Oxygen Deficiency Index (ODI) over five years; Timeseries starts at 1st January 2018 and ends 31st December 2022; Baltic Sea stations (a) FehBB, (b), MePDS, (c) ArkBB, (d) KiellH, according to Table 1; all data for observations taken from MARNET (https://www.bsh.de/DE/DATEN/Klima-und-Meer/Meeresumweltmessnetz/messnetz-marnet_node.html); lack of data might be due to maintenance and/or malfunction of the platform and/or sensor.

340

3.3 Forecasting potential of the ODI?

When plotting both timeseries, the ODI and the observational data over the five years' time span, apparently, we can already visually see seasonality and/or cycles in the observations, as well as in the ODI (Figure 5 and Figure 6). In order to test for the potential of the ODI to forecasting the development of ODZs we applied so called 'lags', which are given by a fixed amount of passing time, in our case days. We plotted the ODI against the lagged observational data and tested lags between 5 and 120 days (Table2: lag5 to lag120). Lagging the observational data means that we shifted the timeseries backwards for the lag amount of the passed days. Like this we plot observational data that happened later in time against the ODI, whose start date we kept static to the 1st January of each corresponding year. In the supplement we exemplarily show each annual timeseries of all 5 years at KiellH. We could identify well defined time-window regarding the ODI33rev configuration between 45 and 75 days, where the probability of forecasting ODZs is significantly higher when compared to lag 120 (Supplement Figure 2 and Supplement Table 4, ODI33rev configuration). After that, we applied the same procedures to the penta-year time series., and results show, that lag60 at KiellH, followed by lag75 and lag45 indicate the highest probability to develop and ODZ (Figure 6d and Table 2). This is in agreement with the annual timeseries at KiellH exemplarily shown in the supplement 120 (Supplement Figure 2 and Supplement Table 4, ODI33rev configuration).

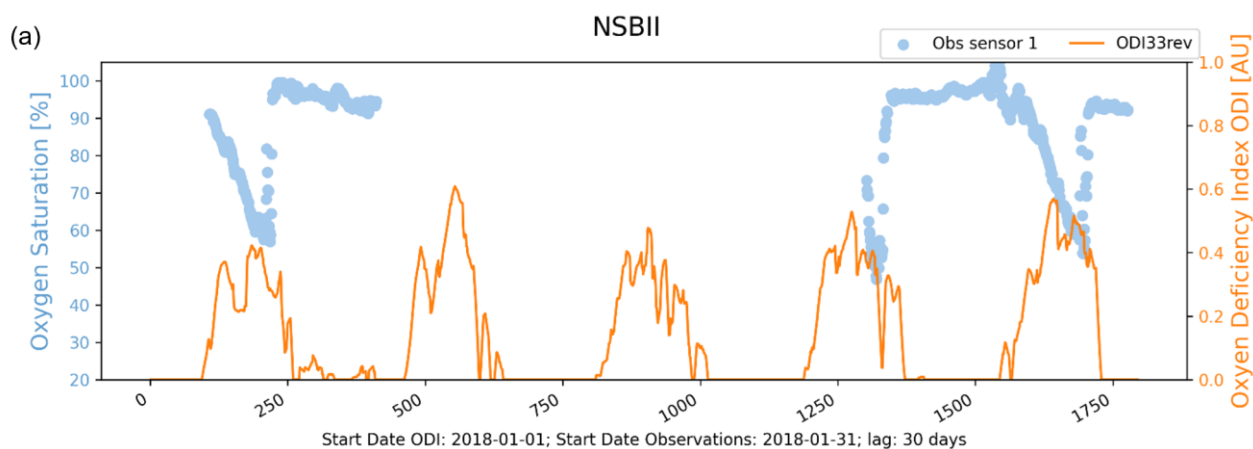
350

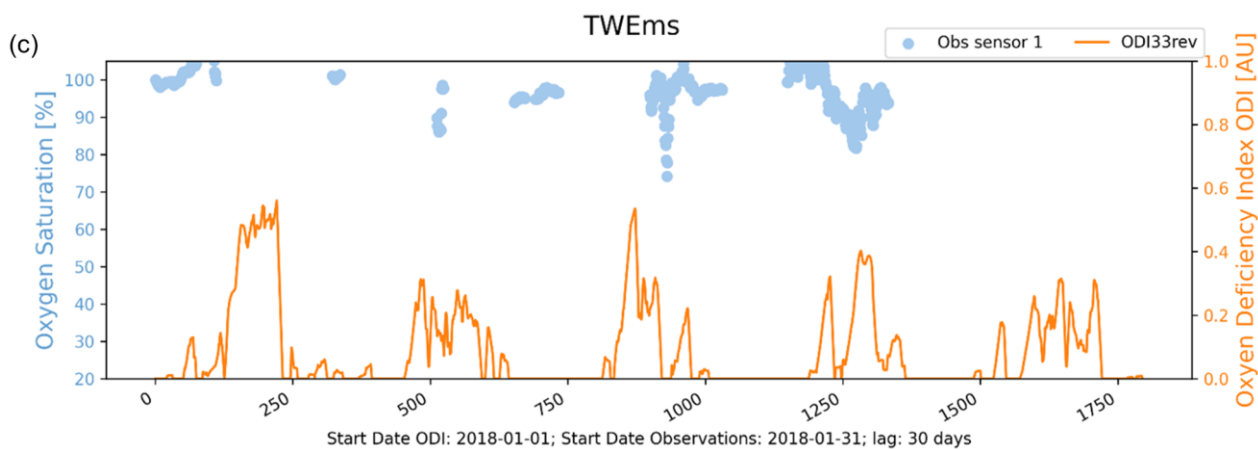
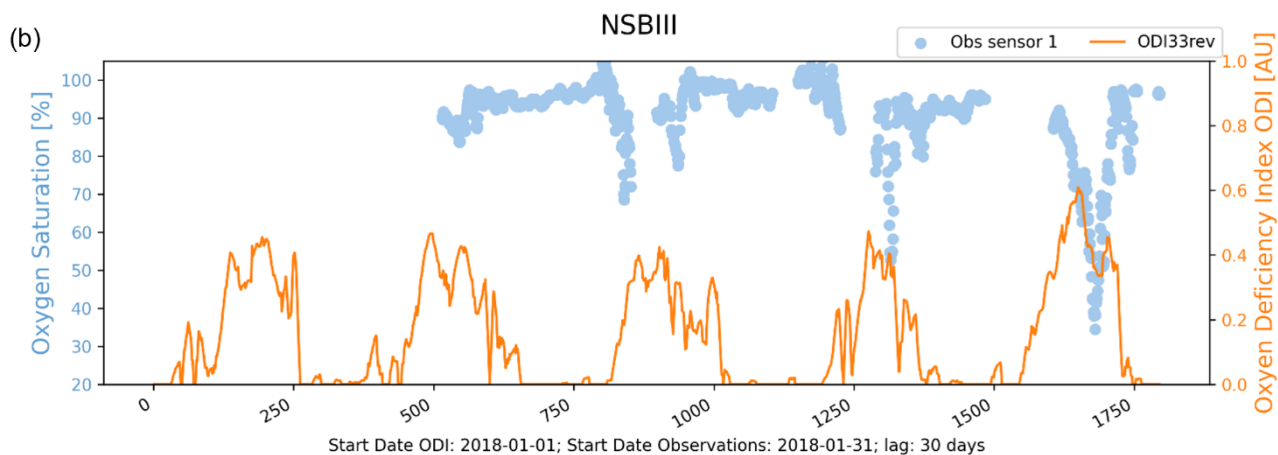
355

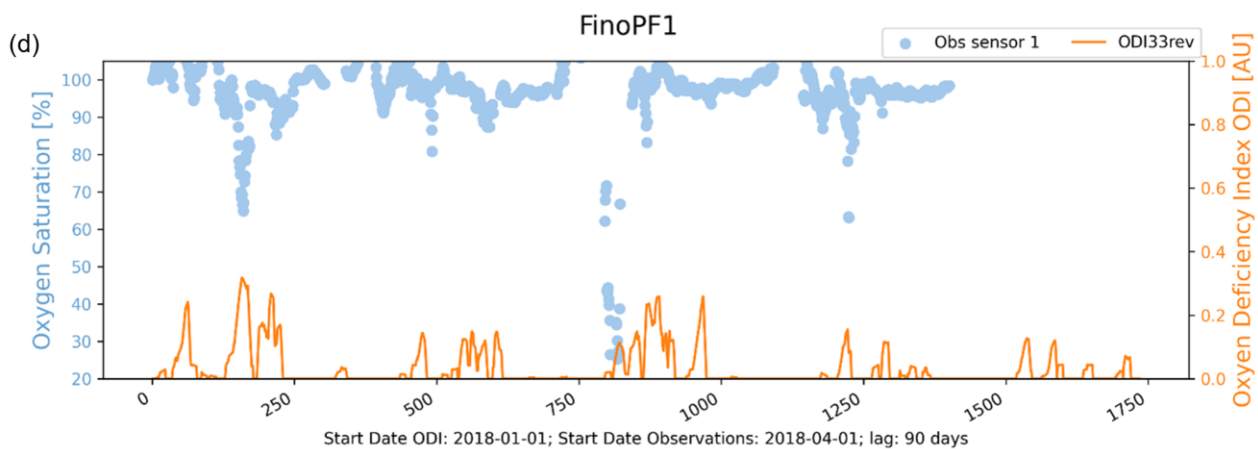
All correlation coefficients improve when lagging the observations against the ODI, but improvements are generally slightly higher at the Baltic Sea, than at the North Sea platforms, except FinoPF1 which increased at lag90 more than 400%, when



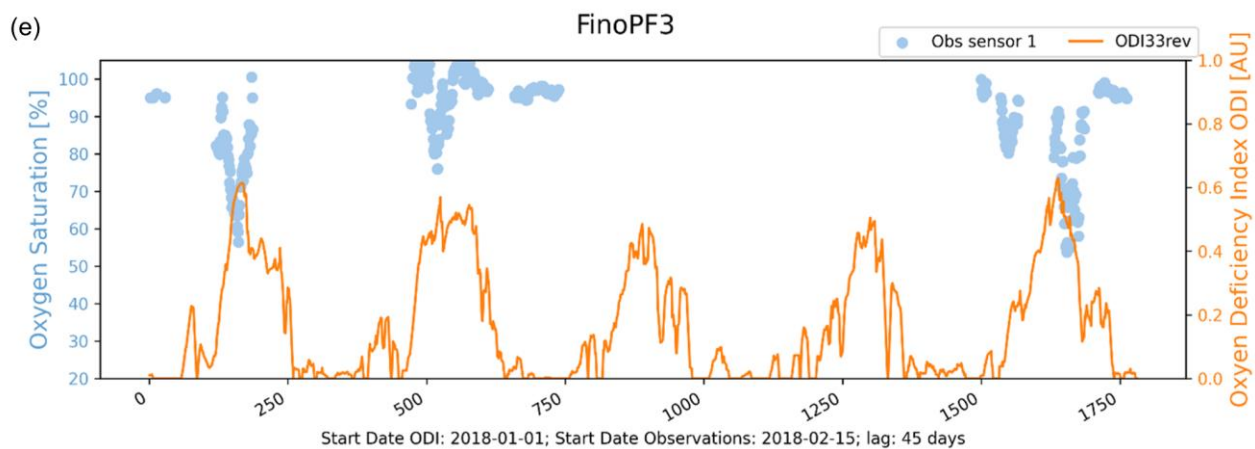
360 compared to lag0 (Table 2). Moreover, in contrary to the North Sea, the highest improvement of the relationship between the
 ODI and the observational data timeseries in the Baltic Sea are rather seen in the later lags (Table 2: respectively), starting at
 60 days (KielBB and FehBB,), 75 days (MePDS) up to 105 days (ArkBB). Moreover, at platform ArkBB the positive
 correlation turned negative after lag10, but is still considered as weak ($r = -0.29$; Table2: lag105). Moderate negative correlation
 coefficients show MePDS ($r = -0.51$; Table2: lag75) and FehBB ($r = -0.54$; Table 2: lag60), whilst KielBB has the highest
 negative correlation coefficient ($r = -0.70$; Table 2: lag60) in the Baltic regime which we consider as good. Whilst FinoPF1
 365 has its highest negative correlation coefficient at lag90, it is still the lowest amongst the North Sea platforms. In contrary,
 TWEmS has its highest moderate negative correlation coefficient at lag5 ($r = -0.41$; Table 2), but barely increased when
 compared to lag0 ($r = -0.35$; Table 2). A special situation can be seen at NSBIII, which shows two equally moderate negative
 correlation coefficients, one at lag30 and the other one at lag60 ($r = -0.58$; Table 2) with a slightly decline in-between at lag45
 ($r = -0.57$; Table 2). Also, moderate negative coefficients have FinoPF3 ($r = -0.40$; Table 2: lag45) and GB ($r = -0.53$; Table 2:
 370 lag30). The highest negative correlation coefficient amongst all platforms is given by NSBII at lag30 ($r = -0.72$; Table 2).
 Panels a-j of Figure 7 show the graphical output to this paragraph.

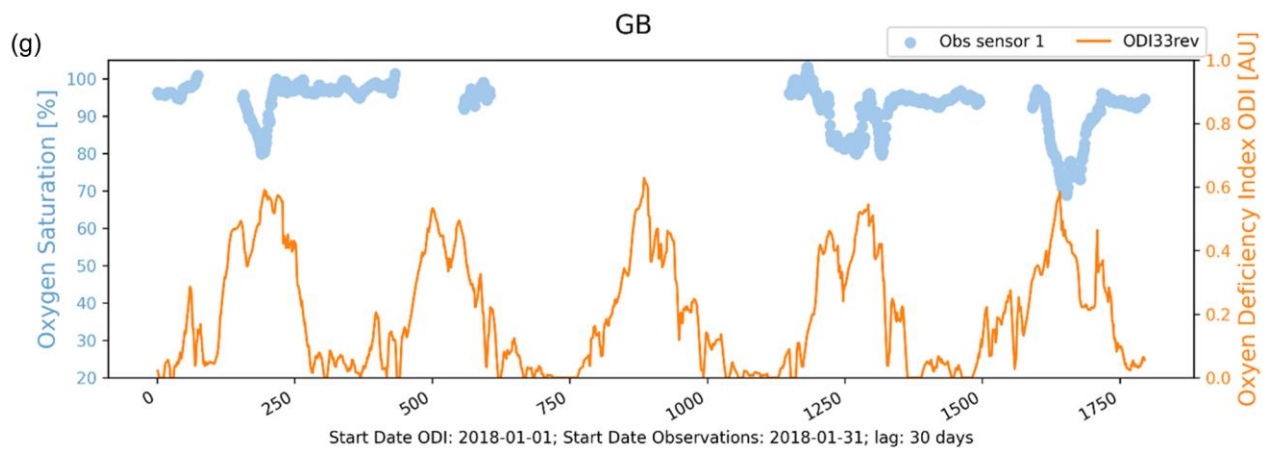
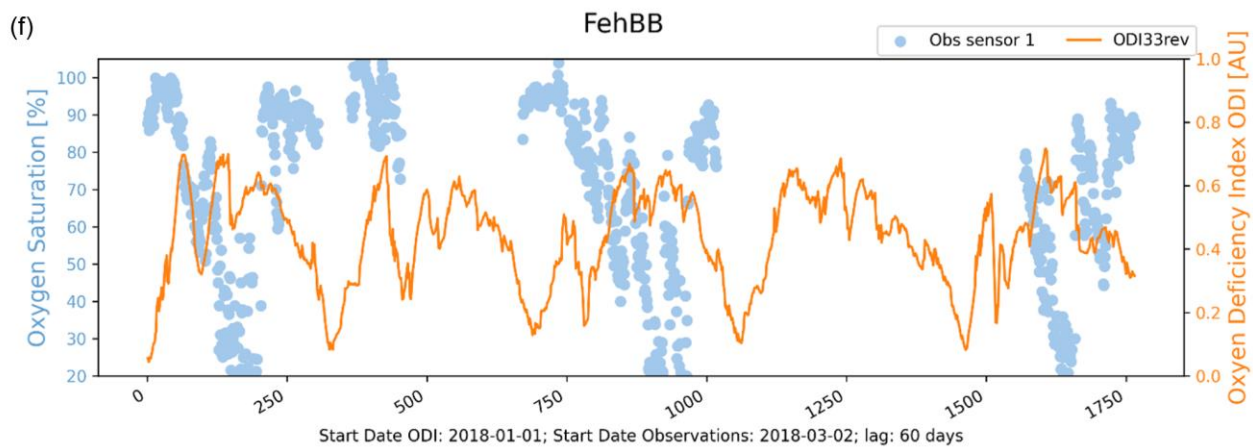


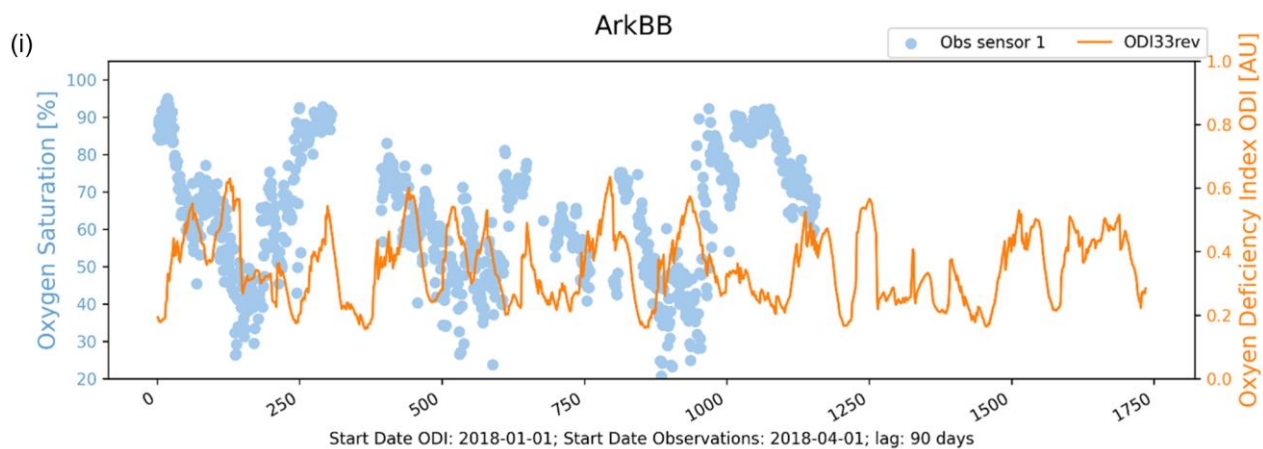
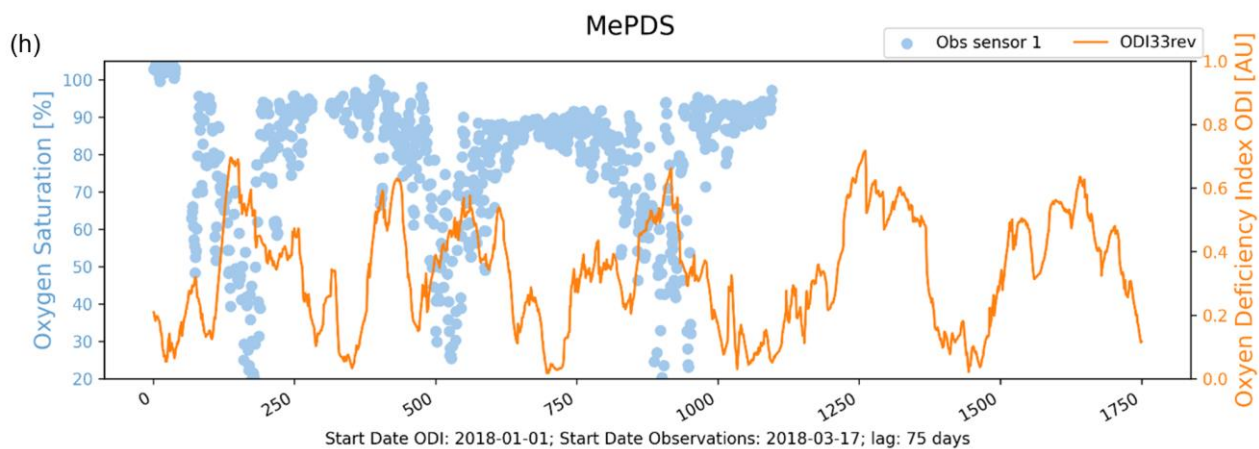




375







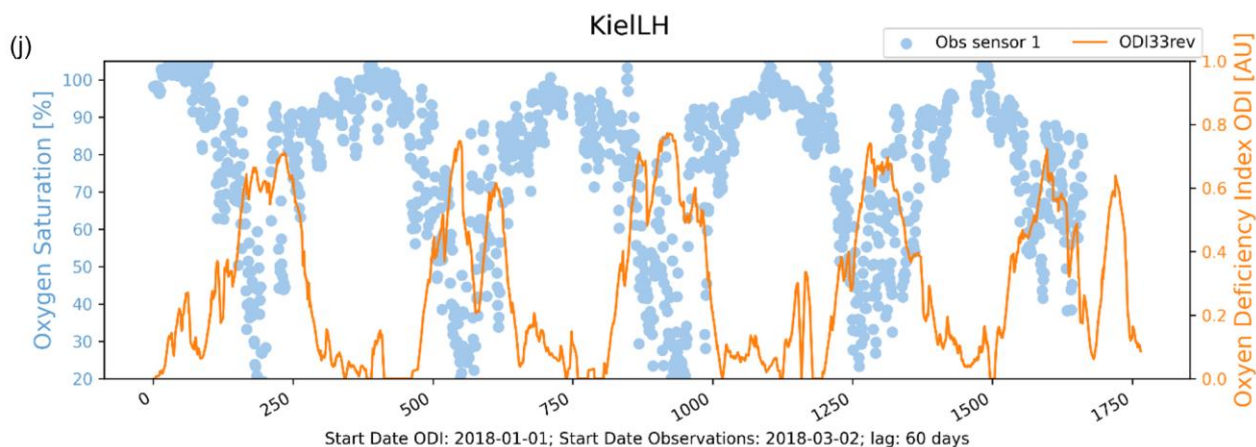


Figure 7: Highest correlation coefficients between the lagged (shifted) daily averaged oxygen saturation timeseries at deepest sensor depths (sensor1) and the Oxygen Deficiency Index (ODI) over five years; ODI timeseries starts always at 1st January 2018; North Sea stations (a) NSBII, (b), NSBIII, (c) TWEmS, (d) FinoPF1, (e) FinoPF3, (f) GB and Baltic Sea and Baltic Sea stations (g) FehBB, (h), MePDS, (i) ArkBB, (j) KielLH, according to Table 1; all data for observations taken from MARNET (https://www.bsh.de/DE/DATEN/Klima-und-Meer/Meeresumweltmessnetz/messnetz-marnet_node.html); lack of data might be due to maintenance and/or malfunction of the platform and/or sensor.

385

Table 2: Pearson's Correlation Coefficients (Corr Coef) between Oxygen Deficiency Index (ODI33rev) and the observed oxygen saturation of sensor 1 at each station the ODI Lag values display the number of days by which the observations were shifted forward in time, see exemplary Figure 5,6 and 7.

390

Station (sensor 1)	ODI	lag0	lag5	lag10	lag15	lag30	lag45	lag60	lag75	lag90	lag105	lag120
MePDS	ODI33rev	-0.32	-0.31	-0.30	-0.32	-0.36	-0.47	-0.50	-0.51	-0.44	-0.32	-0.12
ArkBB	ODI33rev	0.16	0.09	0.03	-0.02	-0.06	-0.06	-0.09	-0.18	-0.28	-0.29	-0.20
FehBB	ODI33rev	-0.35	-0.36	-0.37	-0.38	-0.43	-0.48	-0.54	-0.53	-0.50	-0.43	-0.32
KielLH	ODI33rev	-0.39	-0.45	-0.51	-0.55	-0.62	-0.66	-0.70	-0.69	-0.57	-0.40	-0.23
FinoPF1	ODI33rev	-0.06	-0.12	-0.12	-0.16	-0.11	-0.13	-0.11	-0.09	-0.23	-0.13	0.01
FinoPF3	ODI33rev	-0.32	-0.30	-0.28	-0.25	-0.33	-0.40	-0.35	-0.24	-0.05	0.13	0.20
NSBII	ODI33rev	-0.64	-0.66	-0.70	-0.71	-0.73	-0.72	-0.61	-0.49	-0.35	-0.17	0.03
NSBIII	ODI33rev	-0.47	-0.50	-0.52	-0.52	-0.58	-0.57	-0.58	-0.53	-0.38	-0.23	-0.08
TWEmS	ODI33rev	-0.35	-0.39	-0.38	-0.35	-0.33	-0.39	-0.41	-0.39	-0.35	-0.14	0.01
GB	ODI33rev	-0.48	-0.49	-0.49	-0.50	-0.53	-0.51	-0.48	-0.38	-0.17	0.06	0.18



4 Discussion

In the contrary to a recent study by Piehl et al. (2023), whose using MOM3-ERGOM Model output to assess Oxygen deficiency in the Baltic Sea, by running a postprocessing correction function over modelled oxygen values, our primary goal in this study was not to assess oxygen deficiency in the North and Baltic Seas via the direct outputs of the oxygen parameters from the operational HBM-ERGOM model simulations. Neither, will our current study in first place validate the general HBM-ERGOM model-performance against MARNET observational data. the Oxygen Deficiency Index (ODI) is treated as an independent entity and valuable tool instead that is further used to determine ODZs.

So why we just don't just do something similar with the HBM-ERGOM, which covers the North and Baltic Seas and also includes oxygen dynamics?

Models need calculation and machine time and in the case of complex calculations the model very often has to run on High processing clusters (Piehl et al., 2023). Although, nowadays it is not as difficult as some years ago to get machine time on a high processing cluster to run the model, it is not only pretty expensive in time, but also very often in monetary value. And this exponentially increases with increasing model resolution, parameterization and/or number of days of model forecasts. Moreover, not everybody has the financial support, the expertise and/or the access or even hardware to run a model. Especially in countries with low income these criteria are still a major bottleneck. In the worst case, access to high computing servers might be restricted, denied due to non-complying data policies between the country of origin and the country hosting the servers. Luckily international portals that comply to the Open Data policy, sharing observational and modelling data for free, increased over the last years. This allows to apply postprocessing tools to calculate environmental indicators and make them available to a broader publicity. In our case, we used MARNET near real time data of oxygen saturation monitoring at the 10 stations shown in Table 1.

Here we successfully developed an economic blueprint of the ODI toolbox to identify, scan and forecast oxygen minimum zones, in the North and Baltic Seas. We designed our blueprint, so that the ODI is easily interpretable and usable by several entities, such as Federal Agencies, NGOs and engineers. We discuss briefly the development and pitfalls of the modified ODI. The most striking point during the modification of the ODI are its calculations itself: At no point in this modified ODI formulation, nor in its original formulation after Große et al. (2016), the ODI uses Oxygen to determine ODZs. The ODI is a result of physical and biogeochemical interactions defined in a coupled physical-biogeochemical model, which aims to describe quantitatively and/or qualitatively the interplay between the 'Physics' and the 'Biology'. The better a model is constrained, the better the desired outcome will be (Anderson et al., 2001; Breitburg et al., 2018; Oschlies, 2021; Oschlies et al., 2018; Ward et al., 2019). The better the quality of the data, the longer the time-series, the more reliable the ODI will be. However, if we considered averaged values of NPP and/or fixed values of NPP over a longer period ranging from 1st April to 30th September, a total of 184 days, the performance of the ODI seems to be better (see Tables and Figures in the supplement). However, this improvement comes with a side effect, since the average and/or fixed values of the NPP mimic the finer, noisier



425 ODI fluctuations compared to ODI simulation on a smaller timescale, i.e., our 30 days reference period. We also decided not
to cleanse the data in this study, such as flattening and extrapolating seasonal trends or similar, since the data are scarce and
do have seasonality. We are also aware, that just a good correlation does not explain the causality of the data. Here we only
tested for 10 platforms close to the German shore, in the North and Baltic Seas. Therefore, we want to point out, that the ODI
is still subject of further testing. Thus, we strongly recommend that this blueprint of the ODI tool must not be used alone to
make reliable decisions about the development of upcoming ODZs. Since the data for calculation of the ODI all derived from
430 model output, one might assume that the responsiveness of the unweighted ODI to environmental changes is generally only as
good as the physical and biogeochemical dynamics of the model. However, that the annual fluctuations of low and high oxygen
trends are captured quite well with the ODI, whereas the HBM-ERGOM model strongly underestimates the bottom oxygen
saturation at each station. This might be due to misleading bathymetry data and implementation and/or parametrization of
oxygen fluxes in the HBM-ERGOM model. Nevertheless, we firstly used the modelled bottom oxygen saturation along with
435 modelled bottom oxygen concentration (not shown) at the NSBII, the NSBIII and the TWEmS platform to calibrate our
different approaches of the ODI calculation (Figure 2). This gave us a first hint of the behaviour of the ODI in a more dynamic
oxygen regime with tidal variations and strong hydrodynamics.

Although several hundred stations, frequently monitored in the Baltic Sea
(<https://maps.helcom.fi/website/mapservice/?datasetID=49a98419-f049-47b5-a2e3-ce850fbe2f31>), the oxygen dynamics are
440 very difficult to capture in biogeochemical ecosystem models. For this blueprint we tested the ODI dynamics on a limited
number of platforms. In order to deploy the ODI to different regimes we need to calibrate the ODI with more physical and
biogeochemical data. This will help to strengthen its predictability and forecast ability and to minimize uncertainties for
developing a more robust ODI toolbox. For instance, as it is done with ocean models, the pre-calibration of the ODI can be
done by comparing several model outputs at once, or to use already precompiled multi ensemble model data. These approaches
445 will take into account the seasonal and regional fluctuations, ocean dynamics and ecological constraints. Moreover, we can
use near real time data, or data of cruises, etc. to estimate the ODIs potential to forecast ODZs. A similar approach is used in
the work of Chesapeake Bay (Chesapeake Bay Hypoxia Forecast | Virginia Institute of Marine Science (vims.edu)). Our
modified ODI after Große et al. (2016) has been kept simple and uses the same three controlling parameters. However, our
modified ODI toolbox has been designed for operational use and forecasting ODZs, just as its ‘Grandfather’ - the more
450 complex EUTRISK index - developed by Druon et al. (2004).

Nevertheless, even though in the scarcity of observational data from the ten stations in the Baltic and North Seas, our ODI
captures seasonal dynamics in the observations and in overall we can see, that the ODI displays very well both seasonal
dynamics, winter and spring, in the North and in the Baltic Sea. Its dynamic is in good agreement with the early spring- late
summer phytoplankton blooms, where peaks disappear in the winter months. In contrary at station FehBB, AnkBB and MePDS
455 the ODI levels barely reached the null line, indication of a permanent Oxygen disbalance in those sills (Carstensen and Conley,



2019; Hansson and Viktorsson, 2023). We can see that the ODI in Figure 5 and Figure 6 is somewhat always ahead compared to the observations. Moreover, the ODI also shows clearer seasonal cycles, winter and summer, in the North Sea, than in the Baltic Sea (Figure 5 and Figure 6). Especially at AnkBB the seasons seem to follow rather the canonical calendar seasons, winter, spring, summer and autumn. The winter season is also captured well at NSBIII and at FehBB and KielBB, the values of the ODI are highest and although NSBIII lacks data, all low oxygen peaks are hit by higher ODI values (Figure 5 and Figure 6).

Once we apply lags to compare the oxygen measurements with the ODI, all correlation-coefficients get better (Table 2). In overall the probability of forecasting ODZs in the Baltic Sea more or less doubled, even exceeding 70 % at KielLH. The North Sea improvements are around 10-20% at the monitoring stations (Table 2). FinoPF with its ~400% improvement and TWEmS with basically no improvement, are our outliers. For simplicity we decided to 'manually' shifting data forward or backward in time, instead of using a built-in autocorrelation function. Nevertheless, our investigation provided valuable insights for achieving the best performance of our ODI including an estimate of the number of days in advance for identifying the highest probability/risk of developing ODZs. This kind of low-level forecasts, are pretty constant as shown in the case of KielLH in the supplements. Annual timeseries analyses at KielLH showed the highest probability of developing and ODZ around the 60 to 75 days benchmark, followed by a 45 to 60 days benchmark. Which is confirmed by the 60 days benchmark, when considering the penta-year timeseries (Figure 7).

Also, the improvements of the correlation coefficients in the North Sea are circulated around 30 days, whilst in the Baltic Sea they kick in later (60 days or more) (Table 2). We assume that this might be due to the different hydrographic condition and different time scales of water-masses exchanges with the layers above. Also, we think that the sinking out and decomposition of organic matter at the bottom layers takes some time. Since extreme events, such as storm surges with excessive water movement, would have an immediate effect on the sensor based bottom oxygen saturation, and could be detected due to extreme peaks in the measurements, mixing might be not represented by the calculation of the stratification index when the reference periods are too long, and vice versa. Moreover, Oxygen might drift along the pycnocline with the water movements if velocities or shears inside the stratified layer(s) might be different and therefore the Oxygen might be transported less far away. We assume that, the thinner the layer below the BMLD towards the bottom is, the quicker the Oxygen is consumed and Turbulences might also be less, as they will not be created, due to the limited space. This agrees also with the ability to break the speed of the water transport and limit the exchange of particles and planktonic organisms between denser and less dense water.

We partially deployed graphically our preliminary results of the fixODI33ref together with a visualized estimation of modelled Chlorophyll a data compared to satellite derived Chlorophyll a at the BSH (https://www.bsh.de/DE/THEMEN/Modelle/InfoWas/infowas_node.html). The operational information system at the BSH, regarding the fixODI33rev configuration, only shows areas in proximity around the German coasts of the North and Baltic



Seas to provide more details for the German coastal region. However, we recommend to use these daily outputs with caution and we suggest to evaluate the results of the actual oxygen situation whenever possible with monitoring entities ad loco. Moreover, we found that when employing the different ODI formulations to different regions, the results might get better or worsen. For some regions such as the Baltic Sea, this may reflect that the probabilities of forecasting the developing ODZs become more accurate, whilst for other regions this might not be the case. This also shows, that the ODI blueprint can be easily adapted and modified according to the region-specific needs. In fact, the ODI serves as a blueprint, which should be calibrated for each region and is also subject to personal preferences of the experts (Moriarty et al., 2018).

5 Conclusion

We conclude that the ODI represents the situation of ODZs in the North and the Baltic Seas. Since the ODI valuation is defined for both regimes, which are based on the model output of the operational HBM-ERGOM model of the BSH, we suggest to further test it with other model-configurations (*in prep: Marki et al.*). We also conducted preliminary tests with the operational HBM-ERGOM model coupled to the PDAF framework, where preliminary results have shown that data assimilation improves the correlation coefficients between the bottom oxygen saturation/concentration and the ODI, up to 0.9 (not shown here, *in prep: Marki et al. 2023/2024*). Moreover, we assume that separating spatially the geographical calculation areas of the ODI calculation, and distinguishing the weighting of the single indexes according to the local ecosystems will help to further improve the accuracy and potential of the ODI to forecasting ODZs. This will drive the ODI towards becoming a more robust index that allows for comparison amongst different ecological regimes and over a variety of environmental gradients (Borja and Dauer, 2008). We have shown, that with minimal economic resources it is possible to run the ODI and to forecast the probability of developing an ODZs within a well-defined time-frame, especially to forecasting environmental oxygen conditions that are subject to seasonal transient times at the bottom layers.

Since not every entity whose involved into monitoring oxygen (and/or other environmental parameters) has a scientist at hand who can use a model, we developed a calculation tool, written in Python, which can be applied to several operating systems. Each single module of the Tool can be run independently and uses standard Python packages. There is no need for super-storage or super computing power, although the latter one speeds up the calculations. As long as the input data, of the model or the observations, are Python-edible, we can use other formats than input netCDF files. The code can be easily adapted and publication of the Python based ODI toolbox is intended (Marki et al in prep). Since the output of the ODI is a netCDF File, it can be used with several applications to visualize the output, such as QGIS or other viewers. This will help to strengthen the ODIs forecasting ability, by testing different model outcomes worldwide and in different regimes. Furthermore, this will help to apply automated AI methods to detect environmental threads in advance.



6 Data availability

The monitoring time series data of MARNET stations can be retrieved upon request after registration from the INSITU portal (https://www.bsh.de/EN/DATA/Climate-and-Sea/Marine_environment_monitoring_network/marine_environment_monitoring_network_node.html) and/or upon request via E-Mail from the German Oceanographic Data Center (DOD, dod@bsh.de). HBM-ERGOM operational model outputs can be obtained upon request from the Operational Modelling department at the BSH via E-Mail (opmod@bsh.de).

7 Author contribution

Conceptualization of the ODI blueprint Toolbox was drafted by all authors and with support and suggestions of all our colleagues mentioned in the acknowledgements. All colleagues mentioned in the acknowledgments decided to receive their contribution in the acknowledgement section. AM and XL were responsible for the model data collection. AM was responsible for the monitoring data collection. SJS and AM designed and programmed the final MLD calculation code, and XL and AM programmed the whole Python ODI blueprint toolbox code. AM performed the final simulation and validation experiments and drafted the manuscript. All authors contributed to the improvement of the manuscript by expressing their opinions and recommendations. AM was responsible for the final version of the manuscript, which has been approved for submission by all authors.

8 Competing interests

The contact author has declared that none of the authors has any competing interests.

9 Acknowledgements

This study was supported by the Federal Ministry for Digital and Transport BMDV / German Aerospace Center (DLR RFM), in the framework of the project “InfoWas – Entwicklung eines modellgestützten Informationssystems zur Wasserqualität von Nord- und Ostsee“ (https://www.bsh.de/DE/THEMEN/Forschung_und_Entwicklung/Abgeschlossene-Projekte/InfoWas/infoWas_node.html). We thank our colleagues, LN, AS and SV for collaboration during the InfoWas project. The corresponding author thanks Stephan Krisch for valuable comments and feedback on this manuscript. We thank Fabian Große from the BfG and Fabian Schwichtenberg from the BSH for fruitful discussions. The authors thank Eefke van der Lee, Thorger Brüning and Ina Lorkowski for their support during the InfoWas project (all BSH).



10 References

- 545 Anderson, R., Archer, D., Bathmann, U., Boyd, P., Buesseler, K., Burkill, P., Bychkov, A., Carlson, C., Chen, C. T., Doney, S., Ducklow, H., Emerson, S., Feely, R., Feldman, G., Garçon, V., Hansell, D., Hanson, R., Harrison, P., Honjo, S., Jeandel, C., Karl, D., Le Borgne, R., Liu, K., Lochte, K., Louanchi, F., Lowry, R., Michaels, A., Monfray, P., Murray, J., Oschlies, A., Platt, T., Priddle, J., Quinones, R., Ruiz-Pino, D., Saino, T., Sakshaug, E., Shimmiel, G., Smith, S., Smith, W., Takahashi, T., Treguer, P., Wallace, D., Wanninkhof, R., Watson, A., Willebrand, J., and Wong, C. S.: A new vision of ocean biogeochemistry after a decade of the Joint Global Ocean Flux Study (JGOFS), *Ambio*, 4-30, 2001.
- 550 Bassett, H. R., Stote, A., and Allison, E. H.: Ocean deoxygenation: Impacts on ecosystem services and people, in: *Ocean deoxygenation: Everyone's problem - Causes, impacts, consequences and solutions*, edited by: Laffoley, D., and Baxter, J. M., IUCN, Gland, Switzerland, xxii+562pp, <https://doi.org/10.2305/IUCN.CH.2019.13.en>, 2019.
- Borja, A. and Dauer, D. M.: Assessing the environmental quality status in estuarine and coastal systems: Comparing methodologies and indices, *Ecological Indicators*, 8, 331-337, <https://doi.org/10.1016/j.ecolind.2007.05.004>, 2008.
- 555 Breitburg, D., Levin, L. A., Oschlies, A., Gregoire, M., Chavez, F. P., Conley, D. J., Garçon, V., Gilbert, D., Gutierrez, D., Isensee, K., Jacinto, G. S., Limburg, K. E., Montes, I., Naqvi, S. W. A., Pitcher, G. C., Rabalais, N. N., Roman, M. R., Rose, K. A., Seibel, B. A., Telszewski, M., Yasuhara, M., and Zhang, J.: Declining oxygen in the global ocean and coastal waters, *Science*, 359, 10.1126/science.aam7240, 2018.
- 560 Brüning, T., Li, X., Schwichtenberg, F., and Lorkowski, I.: An operational, assimilative model system for hydrodynamic and biogeochemical applications for German coastal waters, *Hydrographische Nachrichten*, 6-15, 2021.
- Brüning, T., Kleine, E., Janssen, F., Brüning, T., Kleine, E., and Janssen, F.: *Operational ocean forecasting for German coastal waters*, 2014.
- Carstensen, J. and Conley, D. J.: Baltic Sea Hypoxia Takes Many Shapes and Sizes, 28, 125-129, <https://doi.org/10.1002/lob.10350>, 2019.
- de Boyer Montégut, C., Madec, G., Fischer, A. S., Lazar, A., and Iudicone, D.: Mixed layer depth over the global ocean: An examination of profile data and a profile-based climatology, *Journal of Geophysical Research: Oceans*, 109, <https://doi.org/10.1029/2004JC002378>, 2004.
- 565 Doron, M., Brasseur, P., and Brankart, J.-M.: Stochastic estimation of biogeochemical parameters of a 3D ocean coupled physical–biogeochemical model: Twin experiments, *Journal of Marine Systems*, 87, 194-207, <https://doi.org/10.1016/j.jmarsys.2011.04.001>, 2011.
- Doron, M., Brasseur, P., Brankart, J.-M., Losa, S. N., and Melet, A.: Stochastic estimation of biogeochemical parameters from Globcolour ocean colour satellite data in a North Atlantic 3D ocean coupled physical–biogeochemical model, *Journal of Marine Systems*, 117-118, 81-95, <https://doi.org/10.1016/j.jmarsys.2013.02.007>, 2013.
- 570 Druon, J.-N., Schrimpf, W., Dobricic, S., and Stips, A.: Comparative assessment of large-scale marine eutrophication North Sea area and Adriatic Sea as case studies, *Marine Ecology Progress Series*, 272, 1-23, 2004.
- Große, F., Greenwood, N., Kreuz, M., Lenhart, H. J., Machoczek, D., Pätsch, J., Salt, L., and Thomas, H.: Looking beyond stratification: a model-based analysis of the biological drivers of oxygen deficiency in the North Sea, *Biogeosciences*, 13, 2511-2535, 10.5194/bg-13-2511-2016, 2016.



- 575 Hansson, M. and Viktorsson, L.: Oxygen Survey in the Baltic Sea 2022 - Extent of Anoxia and Hypoxia, 1960-2022, SMHI, Report 0283-1112 © SMHI, 2023.
- Huthnance, J., Hopkins, J., Berx, B., Dale, A., Holt, J., Hosegood, P., Inall, M., Jones, S., Loveday, B. R., Miller, P. I., Polton, J., Porter, M., and Spingys, C.: Ocean shelf exchange, NW European shelf seas: Measurements, estimates and comparisons, *Progress in Oceanography*, 202, 102760, <https://doi.org/10.1016/j.pocean.2022.102760>, 2022.
- 580 Laffoley, D. and Baxter, J. M., Laffoley, D., and Baxter, J. M. (Eds.): Ocean deoxygenation: Everyone's problem - Causes, impacts, consequences and solutions., Full Report, IUCN, Gland, Switzerland, 580 pp., <https://doi.org/10.2305/IUCN.CH.2019.13.en>, 2019.
- Levin, L. A. and Gallo, N. D.: The significance of ocean deoxygenation for continental margin benthic and demersal biota, in: Ocean deoxygenation: Everyone's problem - Causes, impacts, consequences and solutions, edited by: Laffoley, D., and Baxter, J. M., IUCN, Gland, Switzerland, xxii+562, <https://doi.org/10.2305/IUCN.CH.2019.13.en>, 2019.
- 585 Maar, M., Møller, E. F., Larsen, J., Madsen, K. S., Wan, Z., She, J., Jonasson, L., and Neumann, T.: Ecosystem modelling across a salinity gradient from the North Sea to the Baltic Sea, *Ecological Modelling*, 222, 1696-1711, <https://doi.org/10.1016/j.ecolmodel.2011.03.006>, 2011.
- MARNET: Oceanographic data from North West Shelf and from the Baltic Sea, dod@bsh.de [dataset], 2018-2023.
- 590 Millero, F. J. and Huang, F.: The density of seawater as a function of salinity (5 to 70 g kg⁻¹) and temperature (273.15 to 363.15 K), *Ocean Sci.*, 5, 91-100, [10.5194/os-5-91-2009](https://doi.org/10.5194/os-5-91-2009), 2009.
- Millero, F. J. and Huang, F.: Corrigendum to "The density of seawater as a function of salinity (5 to 70 g kg⁻¹) and temperature (273.15 to 363.15 K)" published in *Ocean Sci.*, 5, 91–100, 2009, *Ocean Sci.*, 6, 379-379, [10.5194/os-6-379-2010](https://doi.org/10.5194/os-6-379-2010), 2010.
- Moriarty, P. E., Hodgson, E. E., Froehlich, H. E., Hennessey, S. M., Marshall, K. N., Oken, K. L., Siple, M. C., Ko, S., Koehn, L. E., Pierce, B. D., and Stawitz, C. C.: The need for validation of ecological indices, *Ecological Indicators*, 84, 546-552, <https://doi.org/10.1016/j.ecolind.2017.09.028>, 2018.
- 595 Neumann, T.: Towards a 3D-ecosystem model of the Baltic Sea, *Journal of Marine Systems*, 25, 405-419, [https://doi.org/10.1016/S0924-7963\(00\)00030-0](https://doi.org/10.1016/S0924-7963(00)00030-0), 2000.
- Neumann, T., Siegel, H., and Gerth, M.: A new radiation model for Baltic Sea ecosystem modelling, *Journal of Marine Systems*, 152, 83-91, <https://doi.org/10.1016/j.jmarsys.2015.08.001>, 2015.
- 600 Oschlies, A.: A committed fourfold increase in ocean oxygen loss, *Nat Commun*, 12, 2307, [10.1038/s41467-021-22584-4](https://doi.org/10.1038/s41467-021-22584-4), 2021.
- Oschlies, A., Brandt, P., Stramma, L., and Schmidtko, S.: Drivers and mechanisms of ocean deoxygenation, *Nature Geoscience*, 11, 467-473, [10.1038/s41561-018-0152-2](https://doi.org/10.1038/s41561-018-0152-2), 2018.
- Oschlies, A., Duteil, O., Getzlaff, J., Koeve, W., Landolfi, A., and Schmidtko, S.: Patterns of deoxygenation: sensitivity to natural and anthropogenic drivers, *Philos Trans A Math Phys Eng Sci*, 375, [10.1098/rsta.2016.0325](https://doi.org/10.1098/rsta.2016.0325), 2017.



605 Piehl, S., Friedland, R., Neumann, T., and Schernewski, G.: Ocean models as shallow sea oxygen deficiency assessment tools: from research to practical application, *Biogeosciences Discuss.*, 2023, 1-33, 10.5194/bg-2023-152, 2023.

Pörtner, H. O. and Knust, R.: Climate Change Affects Marine Fishes Through the Oxygen Limitation of Thermal Tolerance, 315, 95-97, doi:10.1126/science.1135471, 2007.

610 Schwichtenberg, F., Pätsch, J., Böttcher, M. E., Thomas, H., Winde, V., and Emeis, K. C.: The impact of intertidal areas on the carbonate system of the southern North Sea, *Biogeosciences*, 17, 4223-4245, 10.5194/bg-17-4223-2020, 2020.

Ward, B. A., Collins, S., Dutkiewicz, S., Gibbs, S., Bown, P., Ridgwell, A., Sauterey, B., Wilson, J. D., and Oeschlies, A.: Considering the Role of Adaptive Evolution in Models of the Ocean and Climate System, *J Adv Model Earth Syst*, 11, 3343-3361, 10.1029/2018MS001452, 2019.

615 Zeiler, M., Schwarzer, K., Bartholomä, A., Ricklefs, K., Zeiler, M., Schwarzer, K., Bartholomä, A., and Ricklefs, K.: Seabed morphology and sediment dynamics, 2008.